Flavan-3-ols Are an Effective Chemical Defense against Rust Infection[1][OPEN]

Chhana Ullah,[a] Sybille B. Unsicker,[a] Christin Fellenberg,[b] C. Peter Constabel,[b] Axel Schmidt,[a] Jonathan Gershenzon,[a] and Almuth Hammerbacher[a,c,2]

[a]Department of Biochemistry, Max Planck Institute for Chemical Ecology, 07745 Jena, Germany
[b]Department of Biology and Centre for Forest Biology, University of Victoria, Victoria, British Columbia V8W 3N5, Canada
[c]Department of Microbiology and Plant Pathology, Forestry and Agricultural Biotechnology Institute, University of Pretoria, Pretoria 0028, South Africa

ORCID IDs: 0000-0002-8898-669X (C.U.); 0000-0002-7627-7597 (C.P.C.); 0000-0002-1812-1551 (J.G.); 0000-0002-0262-2634 (A.H.).

Phenolic secondary metabolites are often thought to protect plants against attack by microbes, but their role in defense against pathogen infection in woody plants has not been investigated comprehensively. We studied the biosynthesis, occurrence, and antifungal activity of flavan-3-ols in black poplar (*Populus nigra*), which include both monomers, such as catechin, and oligomers, known as proanthocyanidins (PAs). We identified and biochemically characterized three leucoanthocyanidin reductases and two anthocyanidin reductases from *P. nigra* involved in catalyzing the last steps of flavan-3-ol biosynthesis, leading to the formation of catechin [2,3-trans-(+)-flavan-3-ol] and epicatechin [2,3-cis-(−)-flavan-3-ol], respectively. Poplar trees that were inoculated with the biotrophic rust fungus (*Melampsora larici-populina*) accumulated higher amounts of catechin and PAs than uninfected trees. The de novo-synthesized catechin and PAs in the rust-infected poplar leaves accumulated significantly at the site of fungal infection in the lower epidermis. In planta concentrations of these compounds strongly inhibited rust spore germination and reduced hyphal growth. Poplar genotypes with constitutively higher levels of catechin and PAs as well as hybrid aspen (*Populus tremula* × *Populus alba*) overexpressing the *MYB134* transcription factor were more resistant to rust infection. Silencing *PnMYB134*, on the other hand, decreased flavan-3-ol biosynthesis and increased susceptibility to rust infection. Taken together, our data indicate that catechin and PAs are effective antifungal defenses in poplar against foliar rust infection.

Plant phenolics are a diversified group of secondary metabolites that serve as structural components of plant cells, coloring agents of flowers and fruits, protection against biotic and abiotic stresses, and important agents in human medicine (Treutter, 2005; Pereira et al., 2009; Dixon et al., 2013). Most of these compounds are derived from the aromatic amino acid Phe via the phenylpropanoid pathways. The major subclasses of Phe-derived phenolic compounds include the chalcones, flavones, flavonols, isoflavones, anthocyanidins, proanthocyanidins (PAs), stilbenes, coumarins, furanocoumarins, hydroxycinnamic acids, monolignols, and lignans (Bennett and Wallsgrove, 1994; Kutchan et al., 2015).

PAs (also known as condensed tannins) are phenolics that are major end products of the flavonoid biosynthetic pathway in the tissues of many terrestrial plant species. The building blocks of oligomeric or polymeric PAs are commonly known as flavan-3-ols, which have the characteristic C_6-C_3-C_6 flavonoid backbone (Dixon et al., 2005). Flavan-3-ols differ structurally from other flavonoids by having a nearly saturated C ring with an additional hydroxyl group on the 3-position, which as a chiral center gives rise to cis- and trans-forms of the basic PA-forming units, 2,3-trans-(+)-catechin or 2,3-cis-(−)-epicatechin. The structural diversity of PAs is increased further by the hydroxylation patterns of the B-ring (monohydroxylation, dihydroxylation, or trihydroxylation) and the degree of polymerization (up to more than 100 flavan-3-ol units; Ferreira and Slade, 2002; Hammerbacher et al., 2014).

The biosynthesis of flavan-3-ols and PAs has been studied in many plant species (Xie et al., 2004; Bogs et al., 2005; Paolocci et al., 2007; Pang et al., 2013). The last steps of monomer biosynthesis are catalyzed by two distinct enzymes. For the biosynthesis of 2,3-trans-(±)-flavan-3-ols (e.g. catechin), leucoanthocyanidins are reduced directly to the corresponding flavan-3-ol

[1] This work was supported by the Jena School for Microbial Communication (CUL2014) and the Max Planck Society (GER).

[2] Address correspondence to almuth.hammerbacher@fabi.up.ac.za.
The author responsible for distribution of materials integral to the findings presented in this article in accordance with the policy described in the Instructions for Authors (www.plantphysiol.org) is: Almuth Hammerbacher (almuth.hammerbacher@fabi.up.ac.za).

C.U., S.B.U., J.G., and A.H. designed the research; C.U. performed the experiments and analyzed the data, assisted by A.H.; A.S. produced the transgenic black poplar lines; C.P.C. and C.F. produced the transgenic hybrid aspen lines and conducted the inoculation experiment with the rust fungus *M. aecidiodes*; C.U., J.G., and A.H. wrote the article; all authors read and approved the article.
[OPEN] Articles can be viewed without a subscription.
www.plantphysiol.org/cgi/doi/10.1104/pp.17.00842

(Tanner et al., 2003; Pang et al., 2013) by leucoanthocyanidin reductase (LAR). For the biosynthesis of the 2,3-cis-type compounds (e.g. epicatechin), leucoanthocyanidins are converted to anthocyanidins by anthocyanidin synthase (ANS) and then reduced by anthocyanidin reductase (ANR) to make the corresponding 2,3-cis-flavan-3-ol (Xie et al., 2004). Recently, LAR also was shown to convert 4β-(*S*-cysteinyl)-epicatechin to free epicatechin in *Medicago truncatula* and so plays an important role in regulating the length of PA polymers (Liu et al., 2016). Both LAR and ANR are NADPH/NADH-dependent isoflavone-like reductases belonging to the reductase-epimerase-dehydrogenase superfamily.

Both monomeric flavan-3-ols and PAs have been shown to contribute to plant defense against microbial pathogens, insects, and mammalian herbivores as well as abiotic stresses (for review, see Dixon et al., 2005). Especially in woody plant species, catechin and PAs accumulate upon pathogen infection and are thought to represent antimicrobial defenses (Barry et al., 2002; Miranda et al., 2007; Danielsson et al., 2011; Hammerbacher et al., 2014; Nemesio-Gorriz et al., 2016). In support of this hypothesis, pretreatment of roots with catechin induced systemic resistance in shoots against the bacterial pathogen *Pseudomonas syringae* (Prithiviraj et al., 2007). Catechin also has been shown to quench bacterial quorum sensing and biofilm formation by inhibiting the quorum sensing-regulated gene expression involved in the production of virulence factors (Vandeputte et al., 2010). Furthermore, catechin and epicatechin have been reported to inhibit the appressorial melanization of the necrotrophic fungus *Colletotrichum kahawae* causing coffee-berry disease (Chen et al., 2006). However, strong evidence for a defensive function, including in vitro and in planta studies, are lacking for most systems. In addition, the spatial and temporal dynamics of monomeric flavan-3-ol and PA accumulation in planta upon challenge with fungal pathogens are not well understood.

Poplars (*Populus* spp.) are widely distributed tree species in the northern hemisphere and are considered good model organisms for woody plant research due to the availability of the complete genome of *Populus trichocarpa* (black cottonwood) and established platforms for genetic, molecular, and biochemical research (Tuskan et al., 2006; Jansson and Douglas, 2007). Poplar species also are economically important plantation trees due to their fast growth, use in bioenergy, pulping, and plywood production (Stanturf et al., 2001), and role in phytoremediation of contaminated soil as well as municipal landfills (Schnoor et al., 1995; Robinson et al., 2000). However, under natural conditions, poplars are challenged by a plethora of microbial pathogens (Newcombe et al., 2001).

Poplar rust fungi (*Melampsora* spp.) are the most devastating foliar fungal pathogens of poplar and cause substantial losses in biomass production (Newcombe et al., 2001; Duplessis et al., 2009). The two most destructive species of rust fungi infecting poplar plantations in North America and Eurasia are *Melampsora medusae* and *Melampsora larici-populina*, respectively (Newcombe, 1996). *Melampsora* spp. are obligate biotrophic fungi belonging to the phylum Basidiomycota (Pucciniomycotina, Pucciniomycetes, Pucciniales, Melampsoraceae). Their heteroecious life cycle is very complex, such that two completely different hosts (poplar and larch [*Larix* spp.]) and five different spore types (uredinia, telia, basidia, pycnia, and aecia) are required for completion of the life cycle. The asexual stage of these fungi occurs during early spring and summer on poplar and is characterized by the formation of yellow pustules on the leaves (uredinia) that produce copious amounts of asexual urediniospores with which the fungus can infect new poplar hosts (for review, see Hacquard et al., 2011). With the availability of the complete genomes of both poplar (Tuskan et al., 2006) and the rust fungus (Duplessis et al., 2011), this system has become an important resource for studying plant-pathogen interactions.

Poplars synthesize and accumulate several classes of phenolic metabolites, including salicinoids (phenolic glycosides), anthocyanins, PAs, and low molecular weight phenolic acids and their esters, in leaves, stems, and roots (Pearl and Darling, 1971; Palo, 1984; Tsai et al., 2006; Boeckler et al., 2011). Salicinoids and PAs are generally the most abundant secondary metabolites and together can make up to 30% to 35% of leaf dry weight (Lindroth and Hwang, 1996; Tsai et al., 2006). Although very little is known about the biosynthesis of salicinoids, advances have been made on research into PA biosynthesis in poplar. Three candidate genes encoding LARs and two genes encoding ANRs were discovered in the *P. trichocarpa* genome (Tsai et al., 2006), and a subset of these genes have been genetically characterized in Chinese white poplar (*Populus tomentosa*; Yuan et al., 2012; Wang et al., 2013). Furthermore, the biosynthesis and accumulation of PAs have been shown to be transcriptionally regulated either positively or negatively by MYB transcription factors that have been characterized in poplar (Mellway et al., 2009; Yoshida et al., 2015; Wang et al., 2017). However, biochemical characterization of poplar LAR or ANR proteins catalyzing the two different branches of flavan-3-ol biosynthesis, and regulatory studies of the corresponding genes, have not been attempted so far in black poplar (*Populus nigra*).

Although PAs are constitutively present in poplar species, their biosynthesis can be up-regulated by insect herbivory and mechanical wounding (Peters and Constabel, 2002; Mellway et al., 2009). The role of PAs in defense against leaf-chewing insects is controversial, and these substances have been frequently shown to be ineffective (Hemming and Lindroth, 1995; Ayres et al., 1997; Boeckler et al., 2014). On the other hand, PAs might be an effective defense against pathogen infection. In hybrid poplar (*P. trichocarpa* × *Populus deltoides*), genes of the flavonoid pathway are activated transcriptionally upon infection with the rust fungus *M. medusae*, leading to the accumulation of PAs (Miranda et al., 2007). Overexpression of a PA biosynthetic gene, *PtrLAR3*, in Chinese white poplar increased resistance against *Marssonina brunnea* causing leaf spot (Yuan et al., 2012). However,

further evidence is required to substantiate the function of flavan-3-ols in poplar defense against pathogens.

In this study, we provide evidence that flavan-3-ols are effective chemical defenses in poplar against foliar rust fungus infection. Catechin and PAs, as well as the transcript abundances of the three *LAR* and two *ANR* genes involved in their biosynthesis, increased significantly upon rust infection in black poplar leaves. We also show that these compounds accumulate at the site of infection. In vitro assays using artificial medium amended with physiologically relevant concentrations of catechin and PAs revealed that these compounds are directly toxic to *M. larici-populina*. In planta infection assays using genetically manipulated poplar as well as natural black poplar genotypes with different levels of flavan-3-ols further supported the role of catechin and PAs in the defense of black poplar against pathogen attack.

RESULTS

Catechin and PAs Accumulate in the Leaves of Black Poplar after Rust Fungus Infection

To determine if there is any change in the contents of phenolic compounds in black poplar leaves upon fungal infection, a controlled infection experiment was conducted on young clonal saplings (genotype NP1) using the rust fungus *M. larici-populina*. Poplar plants were inoculated thoroughly by spraying with an aqueous suspension of rust spores, and in parallel, control plants were treated with water. Six fully expanded mature leaves from each rust-infected or control plant were sampled and pooled together (Fig. 1A). The leaf extracts were analyzed by HPLC coupled to diode array detection or fluorescence detection (HPLC-DAD/FLD) or by HPLC coupled to tandem mass spectrometry (LC-MS/MS).

Catechin accumulated in significantly higher amounts (approximately 2.5- to 3-fold) in rust-infected leaves in comparison with uninfected control plants from 3 to 21 d post inoculation (dpi; ANOVA, $P < 0.001$; Fig. 1B). The isomeric epicatechin also accumulated in greater amounts in rust-infected leaves compared with control leaves at 7 dpi (ANOVA, $P < 0.001$; Supplemental Fig. S1), but the concentration was much lower than that of catechin. The concentrations of flavan-3-ol dimers, mainly PA-B1 [2,3-cis-(−)-epicatechin-(4β→8)-2,3-trans-(+)-catechin], increased significantly 2.5- to 3-fold after rust infection (ANOVA, $P < 0.001$; Fig. 1C). We detected and quantified PA oligomers containing flavan-3-ol monomeric size units up to 8 and found that these also increased significantly to a similar degree after rust infection (ANOVA, $P < 0.001$; Fig. 1D; Supplemental Fig. S5). Furthermore, we analyzed the cell wall-bound PAs from the residues after methanol and acetone extractions using the acid butanol method (Porter et al., 1985). Interestingly, the insoluble PAs also accumulated in higher amounts in rust-infected poplar leaves than in the healthy leaves over the course of infection (ANOVA, $P < 0.001$; Fig. 1E). Reductive hydrolysis of soluble PAs into their respective monomeric units revealed that epicatechin and catechin levels increased after rust infection (ANOVA, $P < 0.001$; Fig. 1F).

We quantified other major phenolics in black poplar by HPLC-DAD to determine whether these compounds also accumulate upon rust infection. The concentration of the flavonoid quercetrin increased significantly after rust infection, whereas rutin (quercetin-3-*O*-glucoside-rhamnoside) decreased significantly (ANOVA, $P < 0.001$; Supplemental Fig. S1). Black poplars are well known to synthesize high amounts of salicinoids (Boeckler et al., 2013), which we quantified using HPLC-DAD. Salicin, the simplest salicinoid, accumulated in greater amounts in *P. nigra* leaves after rust infection at 21 dpi compared with uninfected control leaves (ANOVA, $P = 0.017$; Supplemental Fig. S1). However, concentrations of the other salicinoids, salicortin, homaloside D, and tremulacin, decreased in the rust-infected leaves in comparison with the leaves of corresponding control plants (ANOVA, $P \leq 0.005$ for all salicinoids; Supplemental Fig. S1).

To determine the degree of colonization of the fungus in black poplar leaves, we quantified the mRNA levels of the rust *actin* gene and normalized this quantity to the mRNA levels of poplar *ubiquitin* (*PtUBQ*). The abundance of rust fungus in the leaves was low until 3 dpi and then increased exponentially at 7 dpi, coinciding with the appearance of visible symptoms (rust uredia) on the lower surfaces of infected leaves (ANOVA, $P < 0.001$; Fig. 1G).

Three LAR and Two ANR Enzymes Catalyze the Last Steps of Flavan-3-ol Biosynthesis in Black Poplar

To better understand the biosynthesis of flavan-3-ols in black poplar, we utilized the genome of *P. trichocarpa* to identify genes involved in the last steps of the pathway that are specific to flavan-3-ol formation. As identified previously by Tsai et al. (2006), we found three LAR and two ANR candidate protein sequences from *P. trichocarpa* in GenBank and the *Populus trichocarpa* version 3.0 database (Phytozome 11; https://phytozome.jgi.doe.gov/pz/portal.html) using BLAST searches targeting proteome data. The coding sequences of putative *PtLAR* and *PtANR* genes were retrieved from Phytozome, and open reading frames were identified and amplified from *P. nigra* cDNA using primers designed from *P. trichocarpa* mRNA sequences. All three *LAR* and the two *ANR* genes are located on separate chromosomes in the *P. trichocarpa* genome. To investigate the biochemical functions of PnLARs and PnANRs, the genes were cloned and heterologously expressed in *Escherichia coli*. To determine LAR enzyme activity, each *PnLAR* and an apple (*Malus domestica*) dihydroflavonol reductase (*DFR*) gene were coexpressed in *E. coli* cells, and the catalytic activities of the proteins were determined by incubating crude protein extracts with the substrate taxifolin (a dihydroflavonol) and NADPH. The DFR protein converted taxifolin to leucocyanidin, which was then used by

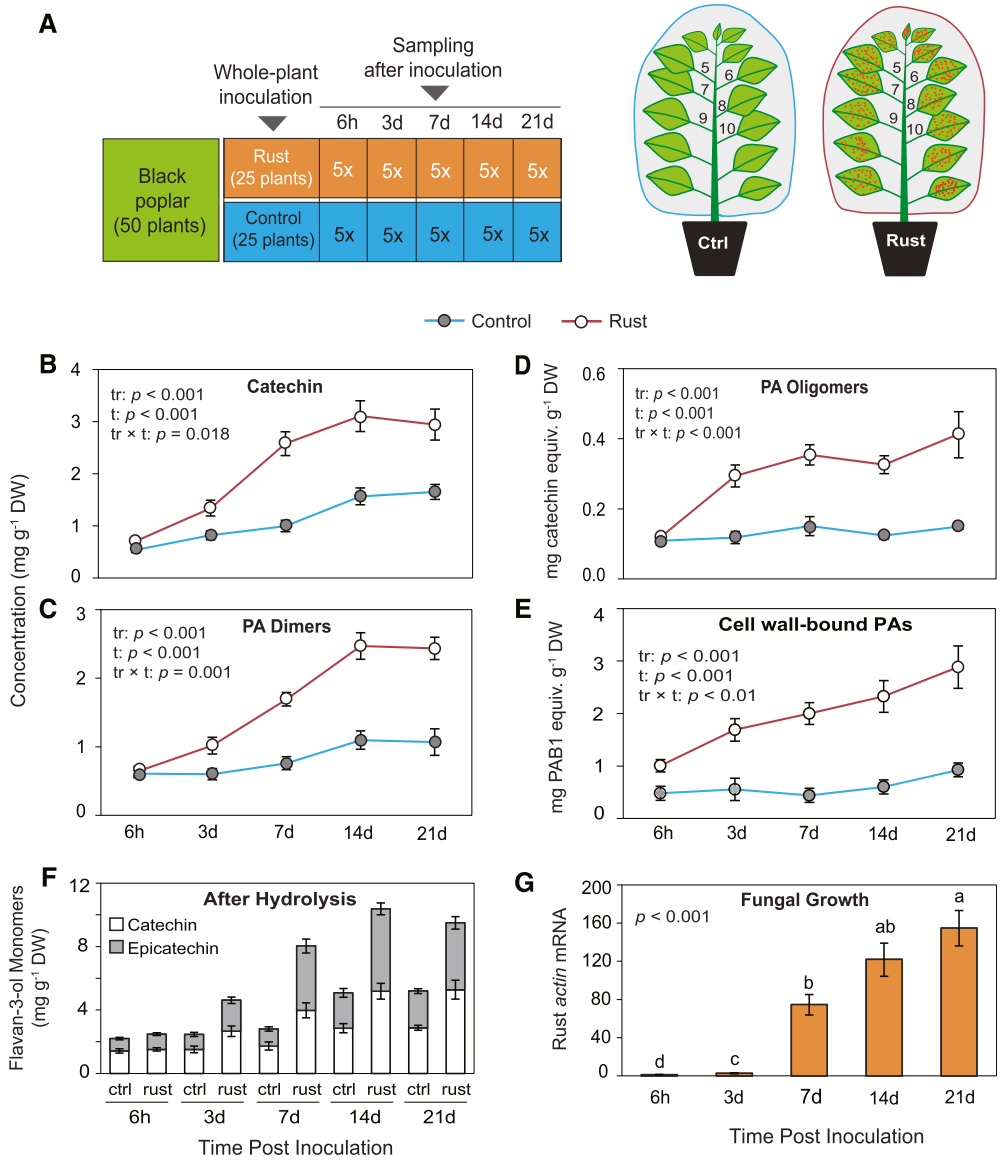

Figure 1. Catechin and PAs accumulate in rust-infected black poplar leaves as antimicrobial defenses. A, Experimental design for controlled inoculation with rust fungus using 50 young black poplar trees (left). At each time point, five plants from each treatment were harvested, with each replicate consisting of the same six leaves from a single plant as depicted (right). B and C, Catechin (flavan-3-ol monomer; B) and PA dimers (C) were measured by LC-MS/MS. D, PA oligomers with up to eight monomeric units were measured by HPLC-FLD. E, Cell wall-bound PAs were measured from the residue remaining after the extraction of soluble catechin and PAs using the butanol-HCl method. The amounts of PA oligomers and cell wall-bound PAs are expressed as catechin and procyanidin-B1 equivalents, respectively. Data were analyzed by two-way ANOVA (factors were as follows: tr = treatment, t = time post inoculation, and tr × t = interaction effect). Corresponding *P* values are indicated in the graphs. F, Composition of flavan-3-ol monomeric units after hydrolytic cleavage of PAs. Metabolite data (catechin and epicatechin) were analyzed separately by two-way ANOVA (tr, $P < 0.01$; t, $P < 0.01$; and tr × t, $P < 0.01$ for both metabolites). G, Colonization of rust fungus in poplar leaves at different times after inoculation. The relative growth of the rust fungus was determined with qRT-PCR by normalizing poplar *UBQ* gene expression to quantify the relative growth of the fungus. Data were analyzed by one-way ANOVA followed by Tukey's posthoc test, and different letters denote statistically significant differences at 95% confidence. Data presented in all graphs are means ± SE ($n = 5$). ctrl, Control; DW, dry weight; rust, rust infected.

all three PnLAR enzymes to make the final product catechin (Fig. 2B). To characterize ANR enzymes, heterologously expressed PnANR was mixed with an expressed *Petunia hybrida* ANS and incubated with the substrate catechin and known cofactors. The *P. hybrida* ANS converted catechin to cyanidin, which was then used as a substrate by both PnANR enzymes to form epicatechin (Fig. 2C).

To determine the evolutionary relationships of the LAR and ANR enzymes from black poplar and other

plant species, a maximum-likelihood tree was constructed (Fig. 3). The closely related protein sequence PtrDFR (an ortholog of apple DFR) was included in the tree. The consensus tree was noticeably bifurcated with two clades: one for all the LARs and the other for all the ANRs. The DFR was more closely related to the ANRs. Within each LAR and ANR cluster, enzymes from gymnosperms and angiosperms clustered separately. The PnLAR3 characterized in this study was closely related to TcLAR (*Theobroma cacao*), with 57% identity at the amino acid level, while PnLAR1 and PnLAR2 clustered with LAR proteins from a range of plant species. LAR1 and LAR2 shared 84% similarity in their sequences at the amino acid level and may have resulted from a recent duplication. Within the ANR cluster, both PnANR1 and PnANR2 clustered together and showed the greatest similarities with MtANR1 (*Medicago truncatula*) and LcANR1 (*Lotus corniculatus*). PnANR1 and PnANR2 share 62% and 64% similarity with Arabidopsis (*Arabidopsis thaliana*) AtANR (AtBAN), respectively, on the basis of their deduced amino acid sequences.

To gain a broader understanding of flavan-3-ol biosynthesis in black poplar at the organ level, we analyzed the constitutive levels of monomeric flavan-3-ols and PAs in leaf laminae, petioles, stems, and roots of 6-month-old black poplar saplings (Supplemental Fig. S2). Concentrations of catechin, PA dimers, and polymers were lower in the leaf laminae than in the stems and roots. Leaf petioles also contained significantly higher

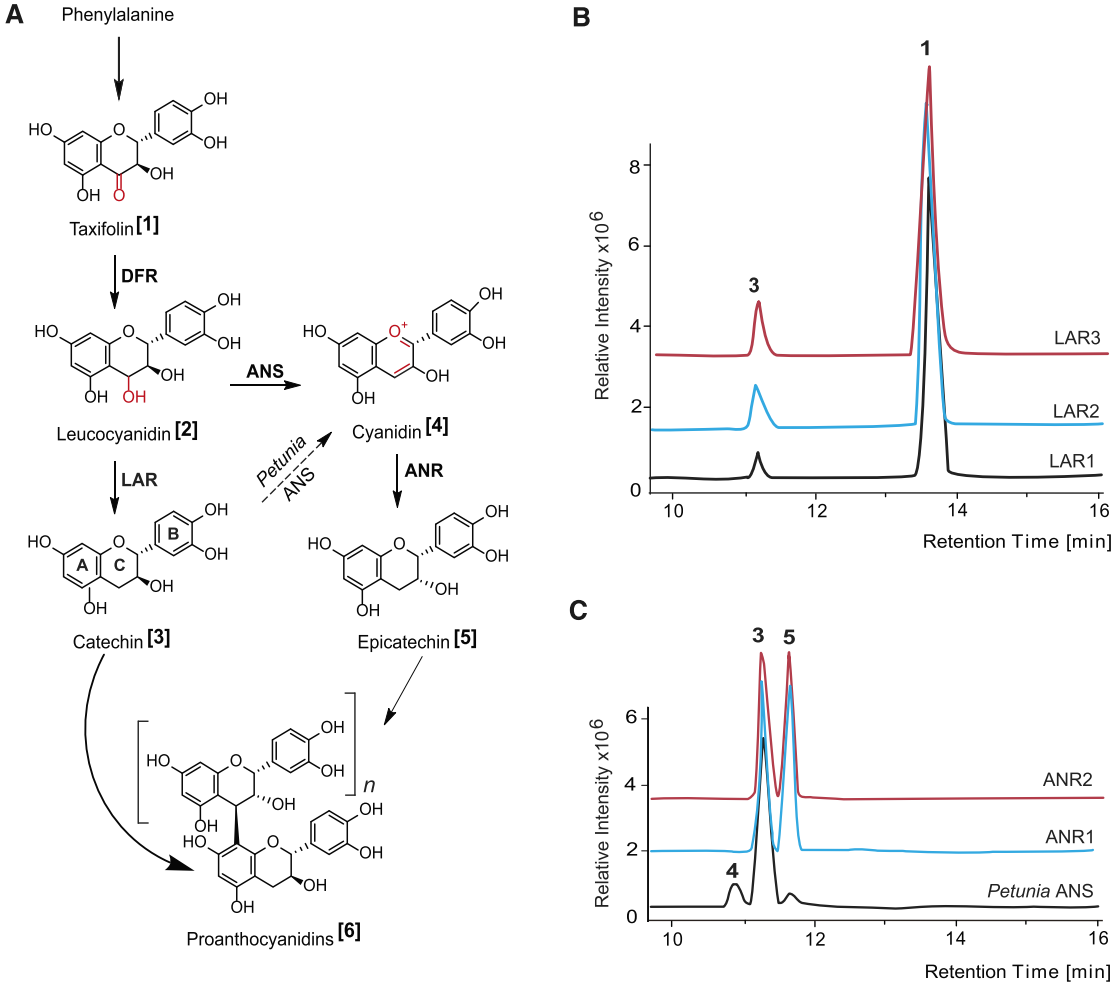

Figure 2. Heterologous expression and biochemical characterization of enzymes involved in the last steps of flavan-3-ol biosynthesis in black poplar. A, Biosynthetic route to monomeric flavan-3-ols and PAs. B, Catalytic activities of LARs. A construct for each *LAR* gene was coexpressed with *MdDFR* in the BL-21 strain of *E. coli*. The crude protein extracts were assayed with taxifolin (a dihydroflavonol) as a substrate. The apple DFR converted taxifolin to leucocyanidin, which was subsequently converted to catechin by the poplar LAR proteins, as measured by LC-MS. C, Catalytic activities of ANRs. Each *ANR* construct was expressed in BL-21, and the crude extract of the expressed protein was used for the enzymatic assay. The crude extract of a *P. hybrida* ANS also was added to each assay, and catechin was added as a substrate (shown with a dashed-line arrow in A). The ANS converted catechin to cyanidin, which was then used as a substrate for the poplar ANRs to produce epicatechin. The numbers on top of the chromatograms correspond to the compounds shown in brackets in A.

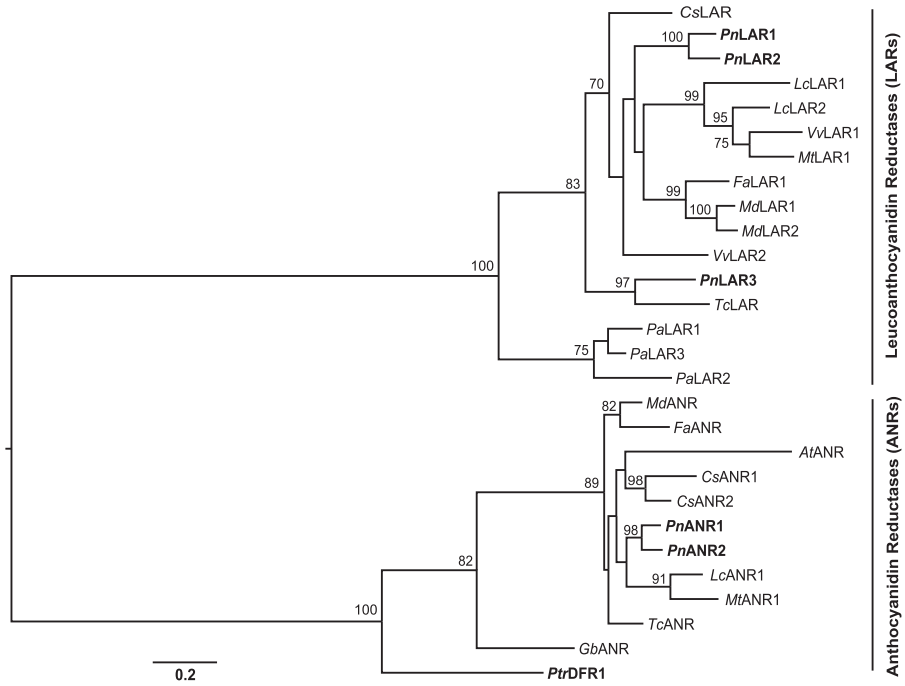

Figure 3. Evolutionary relationship of *LAR* and *ANR* genes of black poplar and other plant species. The corresponding protein sequences were aligned with MAFFT using the L-INS-I method. The maximum likelihood tree was constructed using PhyML-3.1 employing the amino acid substitution model LG (Le and Gascuel, 2008). Nonparametric bootstrap analysis was performed with 1,000 iterations, and values next to each node indicate the branch support percentages (values greater than 70 are included). The scale bar indicates amino acid substitutions per site. The tree was rooted to the midpoint. The peptide sequence alignment is provided in Supplemental Figure S14. Accession numbers of all sequences, including species names, are given at the end of "Materials and Methods."

levels of catechin and PAs than the leaf laminae (Supplemental Fig. S2). The concentration of epicatechin was very low in all parts of the plant (Supplemental Fig. S2). Steady-state transcript levels of the three *PnLAR* and two *PnANR* genes also were measured in different tissues. Transcript levels of *PnLARs* were 2- to 3-fold higher in fully expanded mature leaves and stems in comparison with expanding young leaf laminae and roots (Supplemental Fig. S3). While higher levels of *PnANR1* transcript were found in all leaf laminae than in other tissues (Supplemental Fig. S3), the *PnANR2* was expressed at higher levels in fully expanded mature leaves and older stems (Supplemental Fig. S3).

Increases in Catechin and PA in Rust-Infected Black Poplar Leaves Are Transcriptionally Regulated

To determine if the accumulation of catechin and PAs during rust infection also is transcriptionally regulated in a wild *P. nigra* genotype, we measured the relative transcript abundances of the *PnLAR* and *PnANR* biosynthetic genes characterized in this study as well as *PnMYB134*, an R2R3 domain transcription factor known to regulate PA biosynthesis in poplar (Mellway et al., 2009), by quantitative real-time (qRT)-PCR from the same samples used to measure phenolics. The gene expression data revealed that transcription of the three *PnLAR* genes, the two *PnANR* genes, and the *MYB134* gene was activated after rust fungus infection (ANOVA, $P < 0.001$ for all genes; Fig. 4). *PnLAR* and *PnANR* transcripts increased 3- to 4-fold in the rust-infected leaves at 7 dpi compared with the corresponding control plants (Fig. 4, A–E). Interestingly, the transcription factor PnMYB134 responded quickly after 6 h, with the highest expression at 7 dpi, which is a faster response than for the genes encoding the enzymes of flavan-3-ol biosynthesis (Fig. 4F).

Poplar Genotypes with Constitutively Higher Levels of Catechin and PAs Are More Resistant to Rust Fungus Infection

To elucidate the defensive roles of catechin and PAs in planta during poplar-rust interactions, we tested different poplar genotypes for their susceptibility to *M. larici-populina* infection during June to October 2014. From this preliminary screening, five genotypes ranging from highly susceptible to moderately resistant were then selected for controlled inoculation under natural environmental conditions in summer (June to August) 2015 (Supplemental Table S1).

The constitutive levels of catechin were at least 2 to 3 times higher in the moderately resistant genotypes (Dorn, Kew, and Bla) in comparison with the highly susceptible genotypes (NP1 and Leip; ANOVA, $P < 0.001$; Fig. 5A). All genotypes showed increased levels of catechin in leaves after rust infection (ANOVA, $P = 0.002$; Fig. 5A). The levels of PAs in leaves also were significantly different among the genotypes (ANOVA, $P < 0.001$) and followed the same trend observed for catechin concentration, with moderately resistant genotypes containing higher levels than sensitive genotypes before rust infection and an increase in concentration in response to rust infection (Fig. 5, B and C). Cell wall-bound insoluble PAs also accumulated to higher levels in resistant clones compared with the susceptible clones (ANOVA, $P < 0.001$; Fig. 5D). The minor flavan-3-ols, epicatechin and gallocatechin, did not

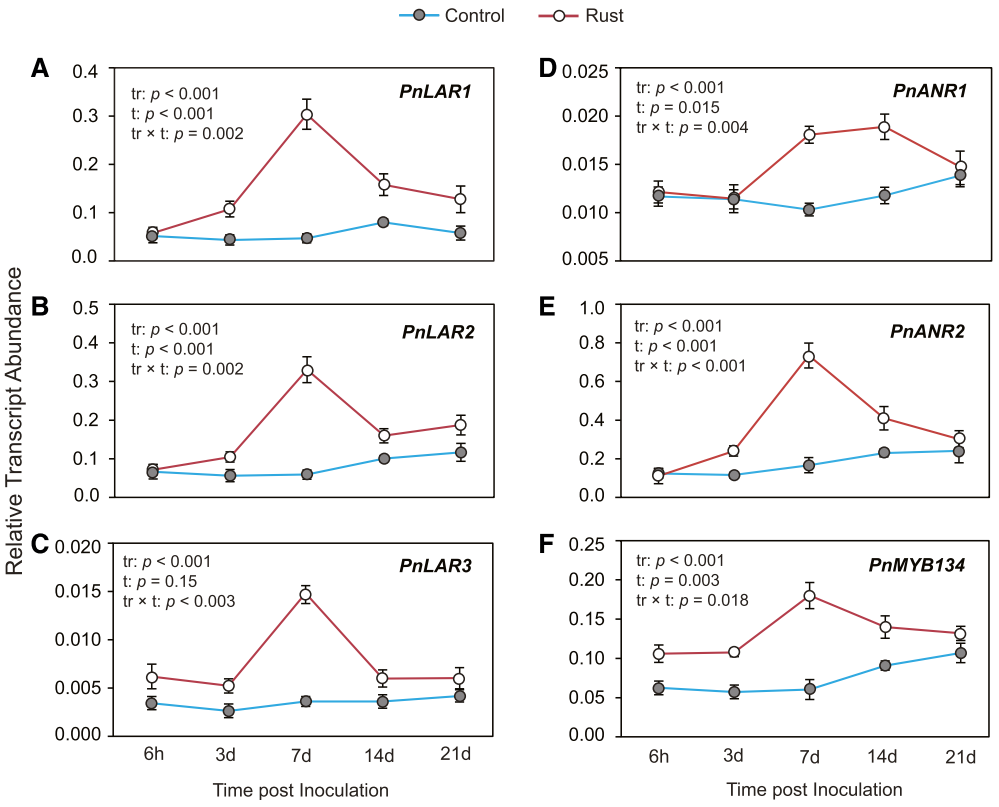

Figure 4. Transcript accumulation of flavan-3-ol biosynthetic genes and a transcription factor regulating PA biosynthesis in *P. nigra* after rust infection. The gene expression of three *PnLAR*s (A–C) and two *PnANR*s (D and E) from *P. nigra* NP1 that were biochemically characterized in this study was measured by qRT-PCR. Gene expression was normalized to *PnUBQ*. Data were analyzed by two-way ANOVA (factors were as follows: tr = treatment, t = time post inoculation, and tr × t = interaction effect). Corresponding metabolite data are depicted in Figure 1. Data represented in graphs are means ± SE ($n = 5$), and each biological replicate consisted of three technical replicates.

change significantly after rust infection (Supplemental Fig. S6). While higher basal levels of epicatechin were found in the susceptible NP1 and Leip genotypes (Supplemental Fig. S6), more constitutive gallocatechins were found in the resistant Dorn, Kew, and Bla genotypes (Supplemental Fig. S6). After acid hydrolysis of PAs, approximately 20% to 30% more gallocatechin and epigallocatechin were recovered in samples taken from the moderately resistant genotypes (Supplemental Fig. S7). Total amounts of flavan-3-ol monomers increased approximately 25% in all genotypes after rust infection 8 dpi (Supplemental Fig. S7). To confirm the resistance of the poplar genotypes to rust fungus infection in this study, we quantified the relative growth of the fungus in rust-infected samples from all five genotypes. The highest rust colonization was found in the genotype NP1, whereas the lowest was found in the Kew and Bla genotypes (ANOVA, $P < 0.001$; Fig. 5E). Transcript levels of two LARs were around 2-fold lower in the susceptible genotype NP1 than in the resistant genotypes, with a significant induction after rust infection. The level of ANR transcripts also was lower in the NP1 and Dorn genotypes than in all other genotypes (Supplemental Fig. S7).

To compare the detrimental effects of rust infection in different poplar genotypes, we allowed a subset of plants of the same age from each genotype to grow under natural conditions for a complete season in 2015. Susceptible, low-flavan-3-ol plants were heavily infected and defoliated by rust damage during mid summer to early autumn (July to September), but plants of the high-flavan-3-ol, moderately resistant genotypes were healthy until November. After seasonal leaf drop in winter, we measured biomass gain in all genotypes. The low-flavan-3-ol genotypes gained 20% to 30% less biomass than the resistant genotypes containing high flavan-3-ols (ANOVA, $P < 0.001$; Fig. 5F). Our results indicated that rust infection can be detrimental to biomass gain over a full growing season, but high flavan-3-ol levels presumably mediate resistance and prevent any decrease in biomass.

Catechin and PAs Are Toxic to *M. larici-populina* in Vitro

To investigate the direct antifungal activities of rust-induced levels of catechin and PAs, an in vitro bioassay was developed for the biotrophic rust fungus *M. larici-populina* (Supplemental Fig. S9). The spore germination and hyphal growth in medium containing the test compounds were monitored with an inverted light microscope. The spores started to germinate after 4 to 5 h of incubation in control medium, but germination was strongly inhibited in medium supplemented with catechin or PAs (Fig. 6, A and B). After 24 h, germinated spores on control slides were highly branched, whereas mycelial branching was inhibited on the catechin- or PA-supplemented slides (Fig. 6, C and D). The germination percentage in control medium was 89.3%, while catechin and PA supplementation significantly reduced germination to 21.1% and 13.3%, respectively (ANOVA, $P < 0.001$;

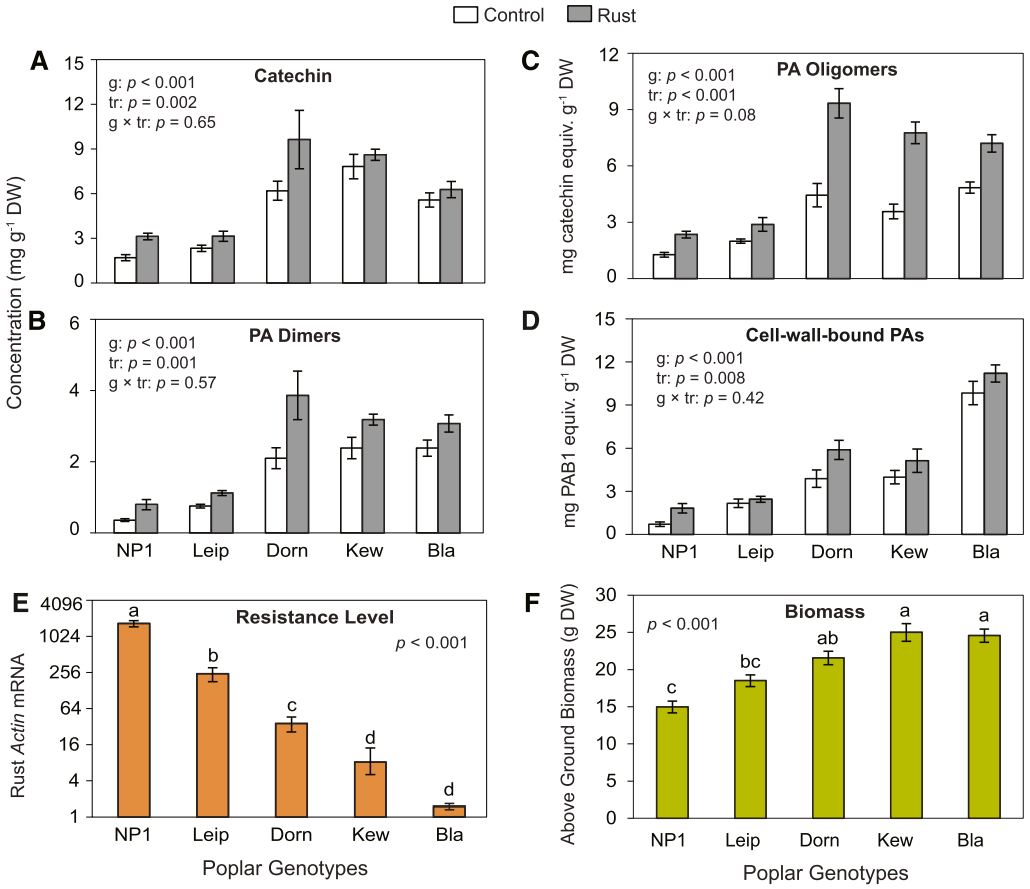

Figure 5. Poplar genotypes moderately resistant to rust fungus contain constitutively higher amounts of catechin and PAs. A and B, Catechin (flavan-3-ol monomer; A) and PA dimers (B) were measured by LC-MS/MS. C, Flavan-3-ol oligomers were measured up to 10 monomeric units by HPLC-FLD. D, Cell wall-bound PAs were measured from the residue remaining after the extraction of soluble catechin and PAs using the butanol-HCl method. The amounts of PA oligomers and cell wall-bound PAs are expressed as catechin and procyanidin-B1 equivalents, respectively. Data were analyzed by two-way ANOVA (factors were as follows: g = genotype, tr = treatment, and g × tr = interaction effect). Corresponding *P* values are indicated in the graphs. E, Fungal growth in different poplar genotypes 8 dpi. The growth of the fungus was determined by qRT-PCR. *M. larici-populina actin* gene expression was normalized to poplar *UBQ* gene expression to quantify the colonization of the fungus in poplar leaves. F, Biomass of poplar genotypes in one growing season under natural environmental conditions. The shoot biomass was determined in autumn (November 2015), when all leaves had dropped at the end of the growing season. In the susceptible genotypes, defoliation was earlier due to severe rust infection. Data in E and F were analyzed by one-way ANOVA followed by Tukey's posthoc test, with different letters indicating statistically significant differences at 95% confidence. Data represented in the graphs are means ± SE ($n = 5$). DW, Dry weight.

Fig. 6E). The average hyphal length on the control slides was 60 μm, while the lengths in the catechin and PA treatments were 17 to 20 μm, respectively (Fig. 6F). Decreased spore germination, reduced hyphal length, and decreased branching on catechin- and PA-supplemented slides indicate that flavan-3-ols are directly toxic to the poplar rust fungus. We also tested different concentrations of catechin and PAs on rust spore germination in vitro. Both catechin and PAs inhibited spore germination at 0.25 mg mL^{-1}, but significant inhibition was observed only from 0.5 mg mL^{-1} (Supplemental Fig. S10). Furthermore, we tested the antifungal activities of epicatechin, salicin, naringenin, and quercetin against *M. larici-populina*. Naringenin inhibited spore germination, but the other compounds did not show any effect on rust spore germination in vitro (Supplemental Fig. S10).

Overexpression of the *MYB134* Transcription Factor in Hybrid Aspen Increased Flavan-3-ol Levels and Reduced Rust Susceptibility

The poplar *MYB134* gene encodes an R2R3 MYB transcription factor and acts as a positive regulator of PAs in poplar. MYB134 overexpression in transgenic *Populus* spp. leads to a strong accumulation of PAs and catechin, but anthocyanins and other flavonoids are minimally affected (Mellway et al., 2009). To directly test the effects of this overaccumulation of flavan-3-ols and PAs on *Melampsora* spp. resistance, we propagated

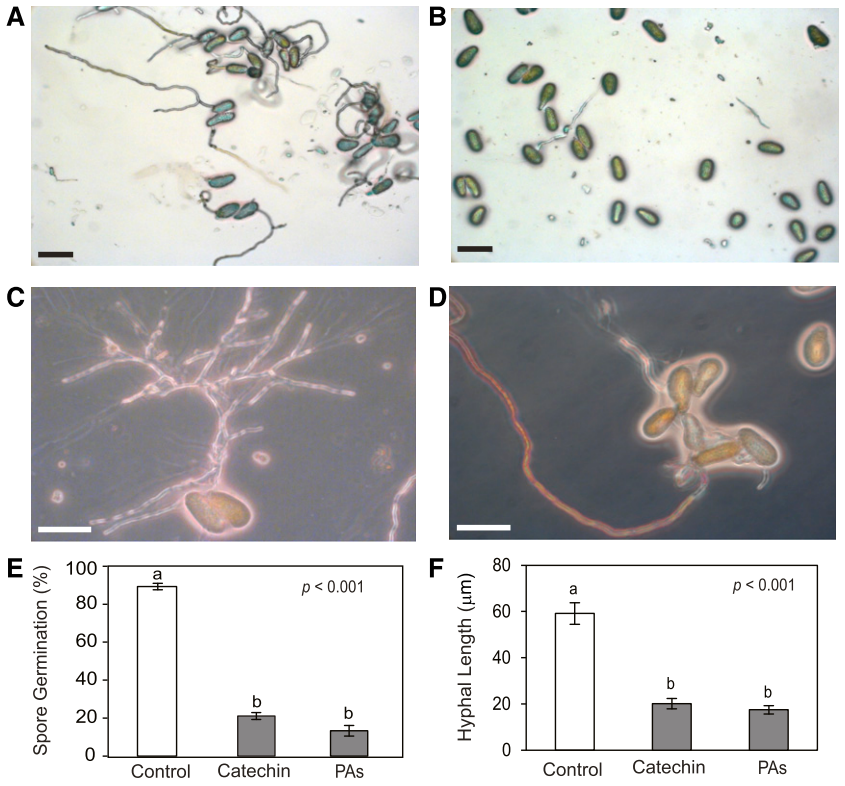

Figure 6. Catechin and PAs show direct inhibitory effects on spore germination and hyphal growth of the biotrophic rust fungus in vitro. A and B, Germination of rust urediniospores on glass slides at 9 h post inoculation (hpi). A, Spore germination shown in control medium. B, Spore germination shown in medium supplemented with catechin. C and D, Patterns of mycelial branching at 18 hpi in control medium (C) and medium supplemented with catechin (D). Bars in A to D = 20 μm. E, Urediniospore germination percentage determined at 9 hpi. F, Hyphal lengths of germinated urediniospores at 12 hpi. Data were analyzed by one-way ANOVA followed by Tukey's posthoc test, and different letters indicate treatment groups statistically different at 95% confidence. Data represented in the graphs are means ± SE (n = 8), where each replicate is a mean of three technical replicates.

three previously characterized hybrid aspen (*Populus tremula* × *Populus alba*) MYB134-overexpressing lines and inoculated these with *Melampsora aecidiodes*, a closely related poplar rust that infects this hybrid. As expected, concentrations of catechin, PA dimers, and PA oligomers were enhanced and up to 3- to 8-fold higher in the MYB134-overexpressing lines (ANOVA, $P < 0.01$; Fig. 7, A–C), and MYB134 expression was 4- to 16-fold higher compared with the wild type (ANOVA, $P < 0.01$; Fig. 7D). To determine rust colonization in the transgenic lines and controls, we quantified *Melampsora* spp. growth using qRT-PCR. Growth of the rust fungus *M. aecidiodes* was reduced significantly in the MYB134-overexpressing lines in comparison with the wild type (ANOVA, $P = 0.002$; Fig. 7E) and roughly inversely proportional to catechin and PA concentrations.

RNA Interference-Mediated Knockdown of *MYB134* Transcription Factor in Black Poplar Down-Regulates Catechin and PA Biosynthesis and Leads to Increased Rust Susceptibility

To complement these findings in black poplar, a native host of the rust fungus *M. larici-populina*, we down-regulated the *MYB134* gene in this species (genotype NP1) by RNA interference (RNAi) to reduce the biosynthesis of flavan-3-ols. We obtained two independent transgenic lines with lower flavan-3-ol monomer and PA levels. Transcript abundances of MYB134 in the MYB-RNAi lines were significantly lower than in the controls (ANOVA, $P = 0.006$; Fig. 8D). The concentrations of catechin, PA dimers, and oligomers were approximately 40% to 50% lower in the RNAi lines in comparison with the vector control and wild-type plants (ANOVA, $P < 0.001$; Fig. 8, A–C). The colonization of infected leaves by the rust fungus was up to 50% higher in the two *PnMYB134*-RNAi lines compared with the vector control and wild-type plants (ANOVA, $P = 0.003$; Fig. 8E). Epicatechin and naringenin concentrations also were significantly lower in the *PnMYB134*-silenced lines (ANOVA, $P < 0.001$), but quercetin did not change ($P = 0.92$). The concentrations of the salicinoids such as salicin ($P < 0.001$), salicortin ($P = 0.02$), and tremulacin ($P = 0.015$) increased slightly in the transgenic lines, but homaloside D ($P = 0.38$) did not change significantly (Supplemental Fig. S11).

Localization of Catechin and PAs at the Site of Rust Infection in Poplar Leaves

During compatible interactions in poplar hosts, rust spores germinate within 6 to 12 h after inoculation and establish an intercellular mycelial network within 2 to 4 d without any visible symptoms (Hacquard et al., 2011). To better understand the role of catechin and PAs against rust infection, we studied their localization in poplar leaves. Tissue-specific localization of PAs was shown in many plant species by staining with 4-dimethylaminocinnamaldehyde (DMACA), which produces a blue color (Kao et al., 2002; Abeynayake et al., 2011; Jun et al., 2015). Histochemical staining with DMACA revealed that catechin and PAs were

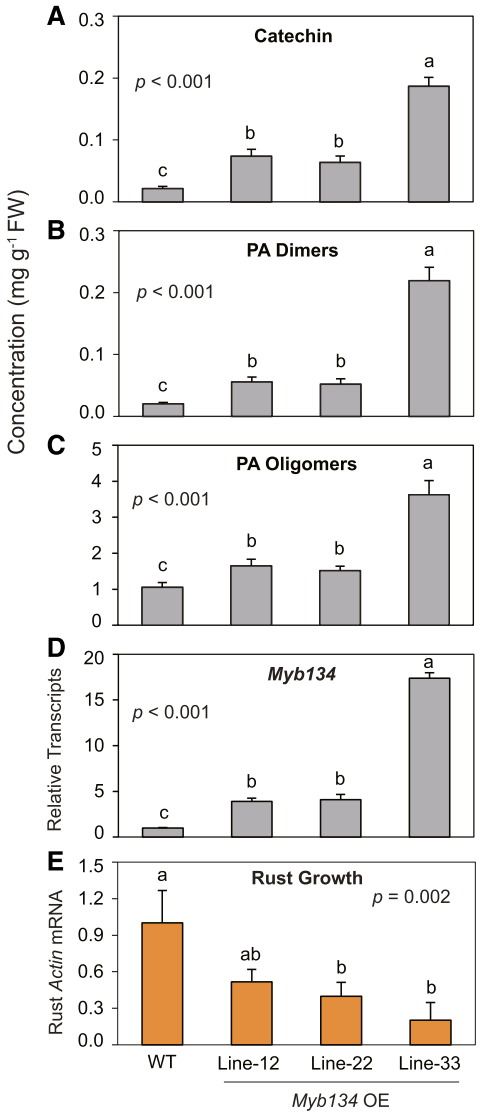

Figure 7. Overexpression of MYB134 in hybrid aspen leads to an up-regulation of flavan-3-ol and PA biosynthesis and reduced *M. aecidiodes* susceptibility. A to C, Concentrations of catechin, PA dimers, and PA oligomers, respectively, in aspen leaves. Catechin and PA dimers were measured by LC-MS/MS, and PA oligomers were measured up to 12 monomeric units by HPLC-FLD. D, Relative expression of *MYB134* mRNA, which was normalized to *UBQ* mRNA levels. E, Relative colonization of the rust fungus *M . aecidiodes* in aspen leaves determined by qRT-PCR. The rust *Actin* mRNA levels were normalized to poplar *UBQ* mRNA to quantify rust colonization. Data were analyzed by one-way ANOVA followed by Tukey's posthoc test, and different letters indicate groups statistically different at 95% confidence. Data represented in graphs are means + SE (n = 5–8). FW, Fresh weight; OE, overexpression; WT, wild type.

densely localized in the upper and lower epidermal layers and vascular bundles of the leaf in rust-resistant poplar genotypes (Fig. 9, C–E). In comparison, a low level of staining was observed in the susceptible genotypes NP1 and Leip (Fig. 9, A and B). After infection with rust fungus, the pattern of flavan-3-ol localization in the leaf changed, with more staining observed in the lower epidermis and near to stomata (site of fungal invasion) and parenchyma cells (Fig. 9, G–K). Staining of leaf petioles from a susceptible genotype revealed that catechin and PAs in this tissue also were localized in the epidermis and vascular bundles (Fig. 9, F and L). Darker staining was observed in the epidermal layer of rust-infected petioles as well (Fig. 9L). Taken together, histochemical staining revealed that catechin and PAs are localized mainly in the epidermis of poplar leaf laminae and accumulate at the site of rust infection. Since poplar synthesizes a variety of salicinoids and flavonoid-derived compounds, we tested the specificity of DMACA. We found that DMACA was very specific to flavan-3-ol monomers and PAs and did not react with other major poplar phenolics (Supplemental Fig. S12).

DISCUSSION

Poplars synthesize a range of ecologically important secondary metabolites, including volatile organic compounds, such as terpenoids, and nitrogenous compounds (Irmisch et al., 2013; Clavijo McCormick et al., 2014) as well as high quantities of phenolic metabolites, including salicinoids, flavonoids, PAs, and hydroxycinnamate derivatives (Tsai et al., 2006; Miranda et al., 2007; Boeckler et al., 2011; Yuan et al., 2012). Although the biosynthesis and antiherbivore activity of these compounds have recently come under close scrutiny (Barbehenn and Constabel, 2011; Boeckler et al., 2013, 2014; Irmisch et al., 2013, 2014), it is still not known if any are effective defenses against pathogens of various lifestyles.

Because chemical defense against plant pathogens has been mostly studied in cultivated rather than wild species and in herbaceous rather than woody plants, we chose to investigate a wild, woody host, black poplar, during its interaction with a foliar rust fungus commonly observed in poplar floodplain forests in Europe. During this study, we assembled comprehensive in planta evidence showing that monomeric (catechin) and polymeric (PA) flavan-3-ols are chemical defenses in poplar against poplar rust (*Melampsora* spp.). Furthermore, we demonstrated that these compounds accumulate preferentially at the site of fungal infection and are directly toxic to this obligate biotrophic fungus at physiological concentrations.

Concentrations of Both Monomeric (Catechin) and Polymeric (PA) Flavan-3-ols Increase in Poplar after Rust Infection

Upon infection with the biotrophic rust fungus *M. larici-populina*, increased levels of catechin and PAs were observed in rust-infected leaf laminae over the course of infection. The isomeric form of catechin, known as (−)-epicatechin, increased in leaves after rust infection. Among the other flavonoids commonly produced by poplar, quercetin increased in rust-infected leaves at the later stages of infection. These results are in agreement with previous studies in poplar, which

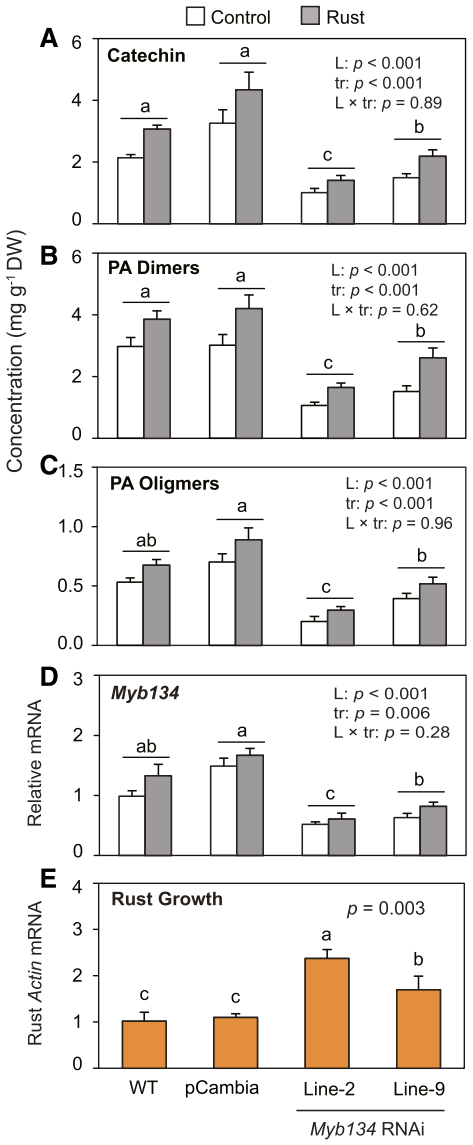

Figure 8. Down-regulation of flavan-3-ol and PA biosynthesis in black poplar (NP1) by silencing the *MYB134* transcription factor results in an increased susceptibility to rust infection (*M. larici-populina*). A and B, Concentrations of catechin and PA dimers, respectively, in poplar leaves measured by LC-MS/MS. C, PA oligomers were measured up to 8 monomeric units by HPLC-FLD. D, Relative expression of *MYB134* mRNA, which was normalized to *UBQ* mRNA levels. E, Relative colonization of rust fungus in poplar leaves determined by qRT-PCR. The rust *Actin* mRNA levels were normalized to poplar *UBQ* mRNA to quantify relative rust colonization. Data in A to D were analyzed by two-way ANOVA (factors were as follows: L = poplar lines, tr = treatment [control and rust], and L × tr = interaction effect) followed by Tukey's posthoc test, and different letters indicate groups statistically different at 95% confidence. Data in E were analyzed by one-way ANOVA followed by Tukey's posthoc test, and different letters indicate lines statistically different at 95% confidence. Data represented in graphs are means + SE ($n = 4–5$). DW, Dry weight; pCambia, vector control; WT, wild type.

showed that several flavonoid biosynthetic genes are transcriptionally activated in poplar after rust colonization, especially during the sporulation phase (Miranda et al., 2007; Azaiez et al., 2009). Studies also demonstrated that the biosynthesis of flavan-3-ols and PAs increased after infection by fungal endophytes in poplar (Pfabel et al., 2012) as well as after infection by pathogenic fungi in other plant species, such as bilberry (*Vaccinium myrtillus*; Koskimäki et al., 2009) and *Fagus crenata* (Yamaji and Ichihara, 2012). Increased accumulation of flavan-3-ols also has been recorded in Norway spruce (*Picea abies*) during infection by necrotrophic fungi (Danielsson et al., 2011; Hammerbacher et al., 2014). Therefore, a range of plants, including poplar, respond to pathogen attack by accumulating both monomeric flavan-3-ols and PAs.

However, not all phenolics increase after pathogen infection. Salicinoids, an abundant class of phenolics in poplar leaves that are known to defend against herbivores (Boeckler et al., 2011), decreased after rust infection, except for salicin, which was induced slightly at the later stages of infection. Thus, salicinoids are not likely to be deployed by poplar for pathogen defense. They might decline because of their metabolism by the fungus as a potential food source; the sugar moiety, in particular, could be cleaved and assimilated by the pathogen (Hammerbacher et al., 2013). A more likely explanation, however, is that lower levels of salicinoids in rust-infected leaves result from elevated flavan-3-ol biosynthesis, which was shown previously to reduce salicinoid biosynthesis. Up-regulation of PA biosynthesis by overexpressing the transcription factor MYB134 led to lower salicinoid content in hybrid poplar (Mellway et al., 2009; Kosonen et al., 2012; Boeckler et al., 2014). In the absence of fungal infection or other biotic stresses, there are typically no dramatic differences in flavan-3-ol or salicinoid concentrations between young expanding and fully expanded mature leaves (Supplemental Figs. S2 and S4; Massad et al., 2014), but this generalization does not apply after herbivore or pathogen attack. In line with previous studies, our phenolic measurements suggest that there is a tradeoff between flavan-3-ol (catechin and PAs) versus salicinoid biosynthesis in poplar leaves (Boeckler et al., 2014), implying a tradeoff between antipathogen and antiherbivore defense.

Transcripts of Flavan-3-ol Biosynthetic Genes Increase in Response to Fungal Infection

The biosynthesis of flavan-3-ols has been well characterized in many plant species, both genetically and biochemically. Two distinct enzymes, LAR and ANR, are involved in catalyzing the last steps of the pathway to flavan-3-ol monomers in PA-producing plants (Bogs et al., 2005; Pang et al., 2013; Liao et al., 2015). Genes encoding LAR and ANR can occur as single genes, for example in Arabidopsis (Xie et al., 2004), or as multigene families, for example in grapevine (*Vitis vinifera*;

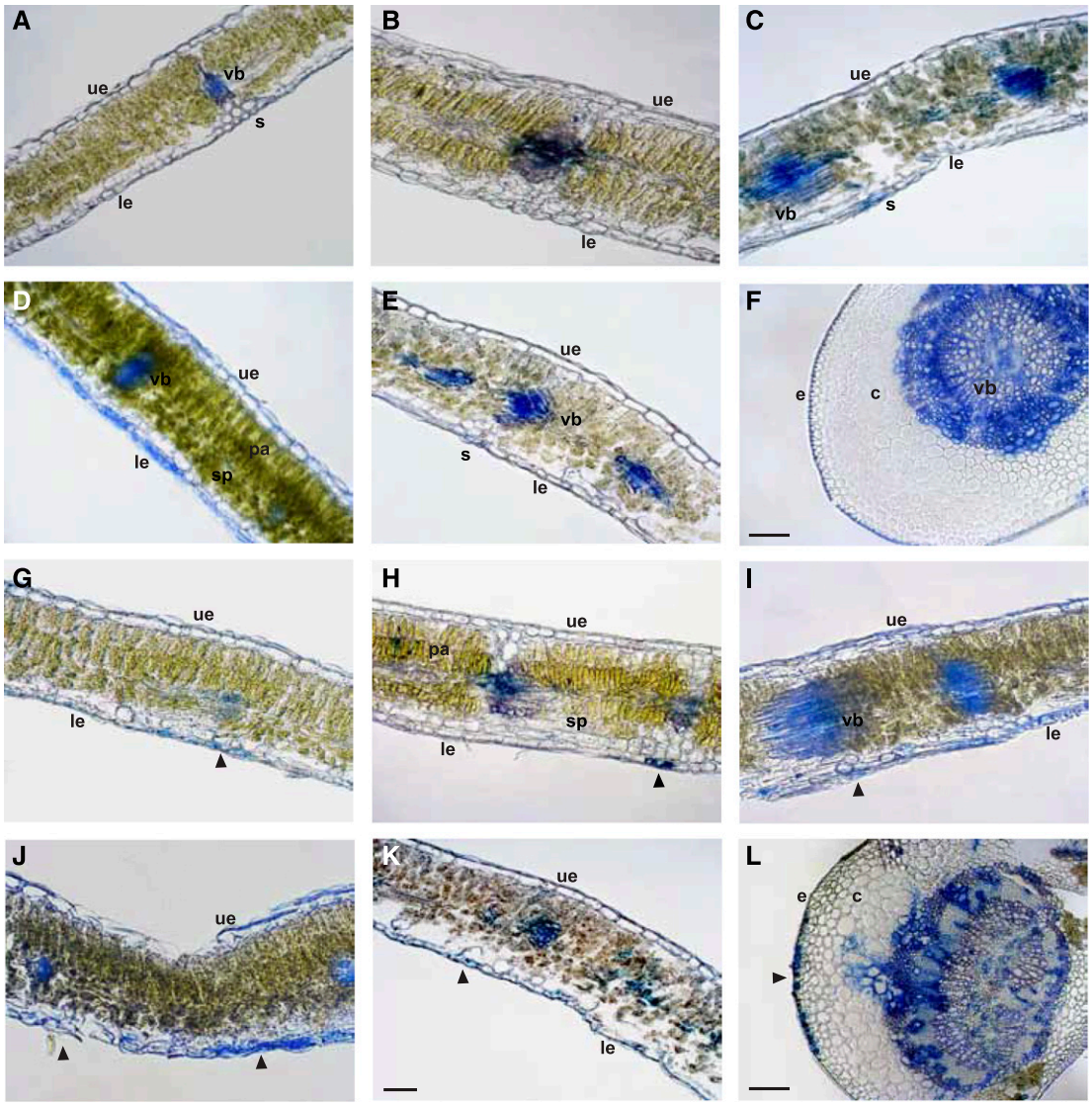

Figure 9. Localization of flavan-3-ols and PAs in poplar leaves with or without rust infection. Sections (20 μm thickness) were made from the first fully expanded mature leaf (leaf 5) and were stained with DMACA. A to E, Cross sections (leaf lamina) of the genotypes NP1, Leip, Dorn, Kew, and Bla, respectively. F, Cross section of an NP1 petiole. G to K, Cross sections (leaf lamina) of NP1, Leip, Dorn, Kew, and Bla genotypes, respectively, after rust infection. L, Petiole cross section of NP1 infected with rust fungus 5 dpi. The genotypes NP1 and Leip were found to be very susceptible to the rust fungus, while the genotypes Dorn, Kew, and Bla were found to be moderately resistant. Triangles indicate fungal penetration and colonization sites. c, Cortex; e, epidermis; le, lower epidermis; pa, palisade parenchyma; s, stomata; sp, spongy parenchyma; ue, upper epidermis; vb, vascular bundles. Bars = 100 μm (K, for all leaf laminae) and 200 μm (F and L).

Bogs et al., 2005) and tea (*Camellia sinensis*; Pang et al., 2013). Analysis of the *P. trichocarpa* genome revealed three loci encoding LAR proteins and two loci encoding ANR proteins. This is more than the two *PtLAR* and one *PtANR* (Yuan et al., 2012; Wang et al., 2013) that were reported previously and genetically characterized in *P. trichocarpa*. We confirmed the enzymatic activity of the proteins encoded by all loci by heterologous expression and in vitro enzyme assays and showed that they are likely involved in the catalysis of the last steps of flavan-3-ol biosynthesis in native black poplar. Our phylogenetic analysis shows that ANRs and LARs are two distinct classes of enzymes and that DFR is more related to ANRs than LARs. Similar evolutionary relationships for ANR and LAR proteins were shown by other authors (Pang et al., 2013; Wang et al., 2013).

Transcript levels of all three *PnLAR* and two *PnANR* genes increased in rust-infected black poplar leaves over the course of infection. Previous microarray data also demonstrated that some of the genes of this pathway are transcriptionally induced in hybrid poplar after infection with *M. medusae* (Miranda et al., 2007). As

reported previously for hybrid poplar (Mellway et al., 2009), the transcription factor *PnMYB134*, a positive regulator of PA biosynthesis, also was transcriptionally induced and responded quickly after rust inoculation in our study. Our transcript and metabolite analyses suggest that both LAR and ANR branches of flavan-3-ol biosynthesis are transcriptionally activated upon rust infection. Monomeric catechin synthesized from the LAR branch is freely available and accumulated in black poplar, while free ANR-dependent epicatechin was observed only at very low concentrations. The recovery of epicatechin after hydrolysis of PAs indicates that epicatechin might contribute to the extension of PA chains. Similar mechanisms also were observed in grape and Norway spruce (Bogs et al., 2005; Hammerbacher et al., 2014).

High Levels of Catechin and PAs Are Associated with Resistance against Rust Fungus Infection

Various constitutive and induced plant phenolic compounds are thought to contribute to defense against microbial pathogens (Osbourn, 1996; Lattanzio et al., 2006), but not all phenolics have this effect (Henriquez et al., 2012; Zhang et al., 2015). In order to determine if flavan-3-ols have this function in planta, we screened five poplar genotypes for resistance against rust infection and quantified their phenolic contents. Interestingly, genotypes moderately resistant to rust infection had constitutively higher amounts of catechin and PAs in their leaves than susceptible genotypes, and substantially higher induced levels of these flavan-3-ols were found after artificial inoculation with rust. Similar results have been shown in other woody plant species. For example, crude extract from coffee (*Coffea arabica*) cultivars resistant to coffee rust (*Hemileia vastatrix*), which contained higher amounts of PAs in comparison with the extracts of susceptible cultivars, was found more effective in inhibiting *H. vastatrix* uredospore germination (de Colmenares et al., 1998). In addition, higher levels of constitutive and induced (+)-catechin were found in a rust-resistant willow (*Salix myrsinifolia*) clone compared with the levels in susceptible clones (Hakulinen et al., 1999). Recently, Wang et al. (2017) showed that *P. tomentosa* increased its PA levels under elevated temperature as well as after infection by the necrotrophic fungus *Dothiorella gregaria*.

To further explore the roles of catechin and PAs as antifungal defenses in poplar, we conducted an infection experiment using *M. aecidiodes* in hybrid aspen overexpressing the *MYB134* transcription factor. Previously, this gene was characterized and shown to be a positive regulator of PA biosynthesis in hybrid poplar and shown to be inducible by biotic and abiotic stresses (Mellway et al., 2009). Rust susceptibility was reduced significantly in MYB134-overexpressing lines accumulating higher levels of flavan-3-ols than the wild-type plants. To investigate the role of catechin and PAs in European black poplar and the rust system, we silenced the *PnMYB134* transcription factor by RNAi in *P. nigra* NP1. We observed a 40% to 60% reduction of monomeric flavan-3-ols and PAs in black poplar after silencing *PnMYB134*. Silenced lines were more susceptible to the rust fungus *M. larici-populina* in whole-plant infection trials (Fig. 8E), confirming the antifungal activity of these compounds in planta. Overexpression of *MYB134* in a hybrid poplar (*P. tremula* × *Populus tremuloides*) caused a significant reduction in salicinoid concentration (Mellway et al., 2009; Boeckler et al., 2014), but such a tradeoff was not observed in the MYB134-silenced *P. nigra* lines accumulating reduced levels of flavan-3-ol and PAs. Silencing of flavan-3-ol biosynthesis is metabolically less costly for poplar than constitutive overexpression or accumulation of flavan-3-ols under pathogen attack. In agreement with our results, overexpression of a PA biosynthetic gene in *P. tomentosa* resulted in increased resistance against necrotrophic fungi (Yuan et al., 2012; Wang et al., 2017). A negative association between fungal endophyte communities and the levels of condensed tannin also was shown in North American poplar species (Whitham et al., 2006). However, infection by necrotrophic fungi was higher in *Populus angustifolia* (Busby et al., 2013), which is known to accumulate high amounts of condensed tannins (Whitham et al., 2006). These conflicting results suggest that poplar-rust interactions are very complex and that other factors, such as pathogen virulence and nonphenolic defenses, including surface immunity and effector-triggered immunity, might contribute to different outcomes of the infection process. Further investigation is necessary using genotypes containing high PAs under natural conditions and also different rust fungus strains.

The Site and Magnitude of Flavan-3-ol Accumulation Are Consistent with a Defensive Role against Fungal Pathogens

The accumulation of flavan-3-ol monomers and PAs often is limited to specific tissue types and developmental stages of plant organs. For example, in white clover (*Trifolium repens*), flavan-3-ol monomers and PAs are localized in the epidermal layers of floral organs (Abeynayake et al., 2011), while in Arabidopsis, PAs accumulate mainly in the seed coat, especially in the endothelial cells (Debeaujon et al., 2003). The biosynthesis and spatial distribution of these compounds in specific tissues or organs might have ecological significance. Our histochemical staining with DMACA revealed that flavan-3-ols are localized mainly in the leaf epidermis and vascular tissues (Fig. 9). Moderately resistant genotypes that contained higher levels of catechin and PAs had a more restricted localization of these compounds in the epidermal layers compared with the susceptible genotypes. After rust infection, high amounts of flavan-3-ols also were observed in the parenchyma cells. The epidermal localization of flavan-3-ols could provide a defensive barrier to early fungal colonization of the leaf. Dark PA staining also

was observed in the lower surface of the aspen leaves (Kao et al., 2002) and in hybrid poplar stems infested by the galling aphid *Phloeomyzus passerinii* (Dardeau et al., 2014).

The effectiveness of an epidermal flavan-3-ol barrier depends on the inhibitory effect of these compounds on rust development. Using a novel in vitro bioassay technique, we showed that physiologically relevant concentrations of both catechin and PAs strongly inhibited rust spore germination and reduced hyphal growth. However, epicatechin did not show antifungal activity even at a 10 times higher concentration than found in poplar leaves (Supplemental Fig. S9), although this compound is an extender unit in PA chains (Fig. 1F). Therefore, our data clearly show that catechin and PAs are active antifungal metabolites in poplar and might serve as an effective chemical defense at the surface or in other tissues of the plant.

In conclusion, black poplar, a perennial woody species of Europe, Asia, and northwestern Africa, was shown to synthesize monomeric and polymeric flavan-3-ols as a phenolic defense against the rust fungus *M. larici-populina* in concentrations demonstrated to have antifungal activity in vitro at sites on the epidermis and in vascular tissue, where they form a barrier to fungal invasion. The rust-resistant poplar genotypes used in this study constitutively accumulate more flavan-3-ols than susceptible genotypes. Transgenic black poplar trees with reduced levels of catechin and PAs were more susceptible. Future work is needed to investigate such topics as the mode of action of flavan-3-ols on fungi, how infection triggers flavan-3-ol accumulation, and if other poplar metabolites act in defense against fungal infection.

MATERIALS AND METHODS

Plant Materials

Black poplar (*Populus nigra*, genotype NP1) was propagated from stem cuttings and grown in the greenhouse (22°C day temperature and 19°C night temperature, 60% relative humidity, 16-h/8-h light/dark cycle) in 2-L pots having a 1:1 mixture of sand and soil (Klasmann potting substrate; Klasmann-Deilmann). Other poplar genotypes were supplied by the Northwest German Forest Research Station in Hannoversch Münden in 2014 as stem cuttings. Plants were regenerated under greenhouse conditions and subsequently multiplied in large quantities. The transgenic black poplar plants used in this study were amplified by micropropagation as described by Irmisch et al. (2013) and then multiplied by stem cuttings. Transgenic hybrid aspen (*Populus tremula* × *Populus alba* INRA 717-1-B4) was grown and maintained as described by Mellway et al. (2009). Plants with a height of approximately 80 to 100 cm were used for inoculation with fungi. Some plants from each genotype were grown outside the greenhouse to allow natural infection by *Melampsora larici-populina*. The disease resistance and susceptibility levels were scored based on the number of uredinia on the abaxial leaf surface as well as by qRT-PCR (a list of genotypes with resistance levels is given in Supplemental Table S1).

Fungal Pathogens and Culture Maintenance

Virulent *M. larici-populina* was collected from a natural population of black poplar located in the floodplain forest of an island in the Oder River near Küstrin-Kietz, Germany. The fungus was multiplied from a single uredium on a susceptible poplar genotype (NP1). The infected plants were covered with polyethylene bags in order to collect spores without allowing any condensation of water inside the bags, which might lead to spore germination. The urediniospores were collected from infected poplar leaves using fine brushes and placed in 2-mL microcentrifuge tubes. To dry spores, the tube was inserted in a closed beaker containing dry silica gel for 2 to 3 d with the cap open. The spores were then stored at −20°C until further use. This spore preservation technique avoided continuous in planta culturing of this obligate biotrophic fungus. Uredospores of *Melampsora aecidiodes* were collected from a local *P. alba* tree.

Inoculation of Poplars with *M. larici-populina* or *M. aecidiodes*

Freshly harvested or frozen urediniospores of *M. larici-populina* were used for inoculation experiments. Young black poplar trees (approximately 80 cm height and 15–20 leaves) grown in the greenhouse were transferred to a climate chamber (22°C day temperature and 19°C night temperature, 70% relative humidity, 16-h/8-h light/dark cycle) 7 d before inoculation. For the kinetic infection experiment, 50 individual black poplar trees of approximately equal size were chosen. Each young potted tree was placed in a separate receptacle (18 cm diameter) for watering independently. Half of the plants (n = 25) were inoculated by thoroughly spraying *M. larici-populina* spore suspension ($\pm 10^5$ spores mL^{-1}) onto the abaxial leaf surfaces. Control plants were sprayed with water (n = 25). Immediately after spraying, each plant was covered with a polyethylene terephthalate bag (Bratschlauch) to maintain high humidity and kept in the dark to facilitate spore germination. After 18 h, the bags were opened from the top to ensure proper aeration. Five time points were chosen for sampling based on the lifestyle of the fungus (Hacquard et al., 2011). Samples were taken at 6 hpi and 3, 7, 14, and 21 dpi. At each time point, five individual plants were sampled from rust-infected and water-sprayed treatments. Six leaves at the same position (leaf 5-10) on each plant were harvested, and midribs were removed and pooled together to obtain one biological sample and immediately flash frozen under liquid N_2. Unless stated otherwise, similar inoculation and sampling techniques were followed for the other rust infection experiments, but only one time point (8 dpi) was used for harvesting leaves. Inoculation of hybrid aspen with *M. aecidiodes* was carried out in the Glover Greenhouse at the University of Victoria using a similar setup.

In Vitro Bioassays with *M. larici-populina* on Glass Slides

Antifungal activities of catechin and PAs against the biotrophic rust fungus were evaluated on glass slides. The germination medium consisted of 1.1% plant agar (Duchefa Biochemie) and 10 mM KCl in water. The medium was sterilized by autoclaving before adding catechin or PAs (1.5 mg mL^{-1}). The media were incubated in a water bath at 65°C for 1 h to ensure that the phenolic compounds were dissolved completely. Autoclaved medium without compounds was used as a control. Approximately 300 μL of liquid medium was pipetted carefully onto a clean glass slide and allowed to solidify. After 5 to 10 min, 20 μL of freshly prepared spore suspension ($\pm 10^4$ mL^{-1}) in 10 mM KCl was pipetted onto the glass slides and spread carefully onto the solidified medium with a plastic inoculation loop. Ten glass slides were prepared for each treatment, and each of them was kept in a sterile petri dish (9 cm diameter) with moist blotting paper to maintain the high humidity required for spore germination. The petri dishes were incubated in a dark cabinet, and the spore germination was monitored every 1 h using an inverted light microscope (Axiovert 200; Carl Zeiss Microscopy) coupled with a camera (AxioVision). The urediniospore germination rate was determined at 9 hpi, and hyphal length was measured at 12 hpi. Three microscopic fields were photographed randomly and considered as technical replicates. The percentage of germinated spores was calculated based on the number of spores germinated divided by the total number of spores observed per microscopic field. Hyphal lengths of the germinated spores in each microscopic field were measured by ImageJ software (https://imagej.nih.gov/ij/index.html). For an illustration of the technique, see Supplemental Figure S8.

Extraction of Phenolic Compounds from Poplar

For the extraction of phenolic compounds, poplar tissues (leaf laminae, petiole, stem, and root) were ground to fine powder under liquid N_2. The stem samples, which contained both bark and wood, were ground with the help of a vibrating mill (Pulverisette 0; Fritsch), while the leaf materials were ground manually using mortar and pestle. The ground samples were lyophilized using an Alpha 1-4 LD Plus freeze dryer (Martin Christ) at 0.001 mbar pressure and −76°C temperature for 2 d. Approximately 10 mg of freeze-dried tissue was

weighed using an XP26 Microbalance (Mettler-Toledo) into 2-mL microcentrifuge tubes. Phenolics were extracted with 1 mL of extraction buffer, which contained 10 μg of apigenin-7-glucoside (Carl Roth) and 0.4 mg phenyl β-D-glucopyranoside (Sigma-Aldrich) as internal standards per 1 mL of methanol (analytical grade). One milliliter of extraction buffer was added to each microcentrifuge tube, vortexed vigorously, and incubated for 30 min at 20°C with shaking at 2,000 rpm. The extracts were centrifuged at 13,000 rpm at 4°C for 5 min, and approximately 900 μL of supernatant was transferred to a new microcentrifuge tube. Salicinoids were analyzed directly with HPLC-DAD. Samples were diluted 20-fold before analyzing flavan-3-ols by LC-MS/MS.

For the extraction of oligomeric or polymeric PAs, approximately 50 mg of freeze-dried plant tissue was extracted with analytical grade methanol following the above extraction protocol, but additionally, the insoluble material was reextracted with 1 mL of 70% acetone. Both supernatants were combined and dried under a stream of nitrogen. The dried samples were redissolved in 1 mL of solvent (1:1, methanol:acetonitrile) and were analyzed by HPLC-FLD. Cell wall-bound PAs were measured from the residue remaining after the extraction of soluble catechin and PAs using the acid butanol method (Porter et al., 1985), which was modified by Boeckler et al. (2013). Amounts of cell wall-bound PAs were determined using a procyanidin-B1 calibration curve (Extrasynthese).

Identification of Phenolics by Liquid Chromatography-Mass Spectrometry with Electrospray Ionization

The phenolic compounds identified from poplar leaf extracts as well as from LAR and ANR enzyme assays were separated on a reverse-phase Nucleodur Sphinx RP18ec column with dimensions of 250 × 4.6 mm and a particle size of 5 μm (Macherey-Nagel) using an Agilent 1100 series HPLC device (Agilent Technologies) with a solvent system of 0.2% aqueous formic acid (A) and acetonitrile (B) at a flow rate of 1 mL min^{-1}. The column temperature was maintained at 25°C. The proportion of B was increased from 14% to 58% in a linear gradient of 22 min. After the column was washed for 3 min with 100% B, it was reequilibrated to the initial eluent composition for 5 min prior to the next analysis. Flow coming from the column was diverted in a ratio of 4:1 before entering the mass spectrometer electrospray chamber. Compound detection and quantification were accomplished with an Esquire 6000 electrospray ionization (ESI) ion-trap mass spectrometer (Bruker Daltronics). Phenolic compounds were analyzed in negative mode scanning a mass-to-charge ratio (m/z) between 100 and 1,600 with a skimmer voltage of 60 V, a capillary exit voltage of −121 V, and a capillary voltage of 4,000 V. Nitrogen was used as a drying gas (11 mL L^{-1}, 330°C), and the nebulizer gas pressure was 35 p.s.i. Compounds were identified by mass spectra and by direct comparison with commercial standards as described previously (Boeckler et al., 2013; Hammerbacher et al., 2014). Bruker Daltronics Quant Analysis software version 3.4 was used for data processing and compound quantification using a standard smoothing width of 3 and Peak Detection Algorithm version 2.

Quantification of Flavan-3-ol Monomers and Dimers by LC-ESI-MS/MS

Chromatography was performed on an Agilent 1200 HPLC system. An API 3200 tandem mass spectrometer (Applied Biosystems) equipped with a turbospray ion source was operated in negative ionization mode. Separation was achieved on a Zorbax Eclipse XDB-C18 column (50 × 4.6 mm, 1.8 mm; Agilent). Formic acid (0.05%) in water and acetonitrile were employed as mobile phases A and B, respectively. The elution profile was as follows: 0 to 1 min, 100% A; 1 to 7 min, 0% to 65% B; 7 to 8 min, 65% to 100% B; 8 to 9 min, 100% B; and 9 to 10 min, 100% A. The total mobile phase flow rate was 1.1 mL min^{-1}. The column temperature was maintained at 25°C. The instrument parameters were optimized by infusion experiments with pure standards as described by Hammerbacher et al. (2014). The ion spray voltage was maintained at −4,500 V. The turbo gas temperature was set at 700°C. Nebulizing gas was set at 70 p.s.i., curtain gas at 25 p.s.i., heating gas at 60 p.s.i., and collision gas at 10 p.s.i. Multiple reaction monitoring was used to monitor analyte parent ion→product ion as follows: m/z 288.9→109.1 (collision energy [CE], −34 V; declustering potential [DP], −30 V) for catechin; m/z 289→109 (CE, −34 V; DP, −30 V) for epicatechin; m/z 304.8→125 (CE, −28 V; DP, −30 V) for gallocatechin; m/z 576.9→289.1 (CE, −30 V; DP, −50 V) for PA B1; and m/z 430.8→ 268 (CE, −46 V; DP, −80 V) for apigenin 7-glucoside. Both Q1 and Q3 quadrupoles were maintained at unit resolution. Data acquisition and processing were performed using Analyst 1.5 software (Applied Biosystems). Linearity in ionization efficiencies was verified by analyzing dilution series of a standard. Flavan-3-ol concentrations were determined relative to the calibration curve for apigenin 7-glucoside as an internal standard and multiplied by the corresponding response factor.

Quantification of PAs by HPLC-FLD

PAs were separated on a LiChrosphere diol column with dimensions of 250 × 4 mm and a particle size of 5 μm (Merck Chemicals) using an Agilent 1100 series HPLC device employing a modified method described previously by Kelm et al. (2006) and Hammerbacher et al. (2014). Briefly, the total mobile phase flow rate for chromatographic separation was 1.2 mL min^{-1}. The column temperature was maintained at 30°C. Compounds were separated using acetonitrile: acetic acid (98:2) and methanol:water:acetic acid (95:3:2) as mobile phases A and B, respectively, with the following elution profile: 0 to 35 min, 0% to 40% B in A; 35 to 40 min, 40% B; 40 to 45 min, 40% to 0% B; and 45.1 to 50 min, 0% B. Eluent was monitored by FLD with excitation at 276 nm and emission at 316 nm. PA oligomer and polymer concentrations were determined relative to the calibration curve for catechin.

Quantification of Other Flavonoids and Salicinoids by HPLC-DAD

To quantify flavonoids other than flavan-3-ols and salicinoids, an Agilent 1100 Series HPLC System with diode array detector (Agilent Technologies) was used. The compounds were separated by a Nucleodur Sphinx RP column with dimensions of 250 × 4.6 mm and a particle size 5 μm (Macherey-Nagel). The solvent system for the mobile phase was Milli-Q water (Millipore) and acetonitrile, but otherwise, the chromatographic conditions were the same as described above for LC-ESI-MS of poplar phenolics. Data were exported by the software Data Trans at different wavelengths for the various phenolics as described previously by Boeckler et al. (2013). For absolute quantification, analyte peak areas were divided by the peak area of the internal standard phenyl β-D-glucopyranoside and multiplied by the corresponding response factors.

Reductive Cleavage of PAs

Reductive cleavage of PAs was carried out as described previously by Hammerbacher et al. (2014). Briefly, the same samples that were used for PA analysis were diluted 50-fold with methanol. The reaction was performed in HPLC glass vials containing 780 μL of diluted extract, 20 μL of trifluoroacetic acid, and 100 μL of sodium cyanoborohydrate (0.5 g mL^{-1} methanol). Reaction mixtures were heated to 65°C for 15 min before adding an additional 20 μL of trifluoroacetic acid. Vials were sealed tightly and incubated overnight at 65°C. The next morning, the reaction was dried completely under a stream of nitrogen, resuspended in 800 μL of methanol, and centrifuged for 5 min at 11,000 rpm at 4°C, and 780 μL of supernatant was transferred to a new vial. The samples were analyzed by LC-ESI-MS/MS as described for flavan-3-ol monomers and dimers.

RNA Isolation and cDNA Synthesis

Total RNA from leaf and stem tissue was extracted using the Invitrap Spin Plant RNA Mini Kit (Stratec Biomedical) following the protocols of the manufacturer, except that an additional DNase treatment was included (RNase-Free DNase Set; Qiagen). The first washing step was conducted with 300 μL of wash buffer R1. After that, DNase (30 Kunitz units in 80 μL volume; 10 μL of RNase-free water and 70 μL of buffer RDD) was added onto the column and incubated at room temperature for 15 min. The column was washed with an additional 300 μL of wash buffer R1 before continuing with the manufacturer's protocol. The quantity and quality of the RNA were checked by spectrophotometry (Thermo Scientific NanoDrop 2000). Reverse transcription of 1 μg of RNA into cDNA was achieved by using SuperScript II reverse transcriptase (Invitrogen) and 50 pmol of oligo(dT)$_{12\text{-}18}$ primer (Invitrogen) in a reaction volume of 20 μL. The cDNA was diluted 5-fold with sterile water, and quality was checked by semiquantitative reverse transcription-PCR using *PtUBQ* primer pairs (primer sequences are given in Supplemental Table S2).

Identification, Cloning, and Sequencing of *PnLAR* and *PnANR* Genes from Black Poplar

The genome of *Populus trichocarpa* (Tuskan et al., 2006) was utilized to find candidate LAR and ANR genes for *P. nigra*, as these two species are closely related. The LAR and ANR protein sequences from apple (*Malus domestica*), grape (*Vitis vinifera*), and tea (*Camellia sinensis*) were used to identify LAR and ANR candidates using BLASTp searches in the National Center for Biotechnology Information and Phytozome version 11 databases. The coding sequences were obtained from Phytozome version 11, and complete open reading frames were identified using the SeqBuilder software of the DNASTAR Lasergene 12 package (DNASTAR). Consistent with Tsai et al. (2006), three *PtLAR* and two *PtANR* genes were identified in the *P. trichocarpa* genome. Gateway (Invitrogen)-compatible primers were designed for candidate sequences by using the 5′ and 3′ ends of putative LAR and ANR genes from *P. trichocarpa* (primer sequences are provided in Supplemental Table S2). Genes encoding LAR and ANR were PCR amplified with Gateway-compatible primers from the cDNA of black poplar using Phusion High-Fidelity DNA Polymerase (New England Biolabs). The PCR products were purified with the QIAquick PCR purification kit (Qiagen). Gateway entry clones were made by using BP Clonase II and pDONR207 (Invitrogen) following the manufacturer's protocol. The pDONR207 constructs harboring *PnLAR* and *PnANR* genes were sequenced using 10 pmol of pDON primers (primer sequences are provided in Supplemental Table S2) and the BigDye Terminator version 3.1 Cycle Sequencing Kit (Thermo Fisher Scientific) on an ABI Prism R 3100 sequencing system (Applied Biosystems). Sequences from each construct were assembled and translated into protein sequences using DNASTAR Lasergene 12 software.

Heterologous Expression of *PnLAR* and *PnANR* Genes in *Escherichia coli*

Three putative *PnLAR* and two *PnANR* entry clones were subcloned with LR Clonase II (Invitrogen) according to the manufacturer's instructions into the Gateway-compatible expression vector pDEST15 (Invitrogen), which contains a GST tag on the N terminus of the expressed protein. All constructs were verified by sequencing with gene-specific primers. A dihydroflavonol reductase gene (MdDFR) from apple, which transforms dihydroflavonols to leucoanthocyanidins (Fischer et al., 2003), also was cloned using the above protocols into the Gateway-compatible expression vector pH9GW, a modified pET28a(+) vector (Novagen), which carries a sequence encoding a 9-His tag at the N terminus of the expressed protein (O'Maille et al., 2004). For *PnLAR* expression, chemically competent *E. coli* BL21 [DE3] (Invitrogen) was cotransformed with the *PnLAR* and *MdDFR* expression constructs. For protein expression, single colonies were inoculated into 5 mL of Luria-Bertani broth with 100 μg mL^{-1} ampicillin and 50 μg mL^{-1} kanamycin for positive selection and grown overnight at 37°C. For *PnANR* expression, BL21 cells were transformed with PnANR expression clones with 100 μg mL^{-1} ampicillin for positive selection and grown overnight at 37°C. The 5-mL starter cultures were used to inoculate 50 mL of overnight expression medium supplemented with their respective antibiotics and grown at 18°C with continuous shaking (220 rpm) for 2 d. The bacterial cells were harvested by centrifugation. The crude proteins were extracted according to Hammerbacher et al. (2014) and used for enzyme assays or stored at −20°C.

In Vitro Enzyme Assays for Functional Characterization of LARs and ANRs

Since the substrates leucocyanidin and cyanidin were not available for LAR and ANR assays, respectively, enzyme assays were conducted using two-step reactions. For LAR characterization, taxifolin was used as a substrate with the coexpressed (PnLAR + MdDFR) crude protein extract. The reactions were performed in a 100-μL reaction volume containing 70 μL of crude protein extract, 10 μL of NADPH (20 mM), and 20 μL of taxifolin (50 mM) for 40 min at room temperature. The reactions were stopped by adding 100 μL of methanol. The mixtures were centrifuged at 11,000 rpm for 4 min, and supernatant was analyzed by an LC-ESI-ion-trap mass spectrometer. For ANR characterization, an ANS gene from *Petunia hybrida* was cloned into pDEST15 and heterologously expressed in *E. coli*, and crude protein was extracted using the protocols described above. The enzyme assay was performed with 200 μL of crude protein extracts (100 μL each of the ANR and ANS) and 10 μL of catechin (10 mM) as substrate. The reaction mixture also contained 20 μL of NADPH (20 mM), 10 μL of oxoglutarate (10 mM), 1 μL of enzyme bovine catalase (40 units mL^{-1}; Sigma-Aldrich), 40 μL of potassium phosphate buffer (0.2 M; pH 6), 10 μL of ascorbate (50 mM), and 1 μL of $FeSO_4$ (1 mM). The reaction mixture was incubated at 28°C overnight. The reaction was stopped by adding another 100 μL of methanol and centrifuged for 4 min at 11,000 rpm, and the supernatant was analyzed by the LC-ESI-ion-trap-MS.

qRT-PCR

To quantify the expression of target genes, a segment of approximately 150 bp was amplified using gene-specific primers. All primers were designed using Primer3 Web version 4.0.0 (http://bioinfo.ut.ee/primer3/). The efficiency of each primer pair was tested before qPCR. Primers with efficiencies below 95% were discarded. The reactions were performed in a 20-μL volume containing 10 μL of Brilliant III Ultra-Fast SYBR Green QPCR Master Mix (Agilent Technologies), 10 pmol of forward and 10 pmol of reverse primer, and 2 μL of diluted cDNA (approximately 100 ng). The qRT-PCR was performed using the CFX Connect Real-Time PCR Detection System (Bio-Rad) using a two-step amplification protocol (cycling parameters: 3 min at 95°C followed by 40 cycles of 10 s at 95°C and 30 s at 55°C). A nontemplate water sample was used as a reaction control. Transcript abundance was normalized to the abundance of the *PtUBQ* (Irmisch et al., 2013) and was calculated from five biological replicates, with each biological sample being analyzed from three technical replicates. Primer sequences for all genes used in this study are given in Supplemental Table S2.

Histochemical Staining and Microscopy

Fresh plant specimens were embedded into Tissue Freezing Medium (Jung, Leica Biosystems) and left for 1 h at −20°C. Sections (10–20 μm) were made using a CM1850 cryotome (Leica Biosystems). Then, two to three sections were transferred to a clean glass slide and stained for 10 min with approximately 50 μL of freshly prepared 1% DMACA solution (1% [v/v] DMACA in absolute ethanol containing 5 N [1:1, v/v] HCl). After 10 min of staining, the excess DMACA solution was wiped off carefully, and one drop of 70% (v/v) glycerol was added to the sections. A clean coverslip was put carefully on the sections and observed using an inverted light microscope (Axiovert 200; Carl Zeiss Microscopy), and photographs were taken with a camera (AxioVision).

Phylogenetic Analysis

Full-length amino acid sequences of LARs and ANRs were retrieved from public databases (GenBank/National Center for Biotechnology Information/EMBL and Phytozome version 11). A poplar DFR protein sequence (ortholog of apple DFR) was included. Protein sequences were aligned using the multiple sequence alignment program MAFFT version 7 (Katoh and Standley, 2013) by employing the highly accurate method L-INS-I (sequence alignment is provided in Supplemental Fig. S13). The aligned sequences were then verified and edited using Mesquite 3.04 (http://mesquiteproject.org). The maximum likelihood tree was constructed using the software package PhyML-3.0 (Guindon et al., 2010). The amino acid substitution model was LG (Le and Gascuel, 2008). A BIONJ distance-based tree was the starting tree by default and then improved by tree topology search by combining Nearest Neighbor Interchange and Subtree Pruning and Regrafting. Bootstrapping was estimated with 1,000 replicates. The tree was viewed using Figtree (http://tree.bio.ed.ac.uk/software/figtree/) and rooted at the midpoint. The tree readability was improved using Adobe Illustrator CS5. The accession numbers of all peptide sequences are given at the end of "Materials and Methods."

Vector Construction and Plant Transformation

The binary vector was constructed following the method described by Levée et al. (2009). The transformation of *P. nigra* NP1 by an RNAi construct was achieved following a protocol optimized for *Populus canescens* (Meilan and Ma, 2006). To target *PnMYB134* mRNA, a fragment between positions 512 and 696 of the coding sequence was selected. Transgenic RNAi poplar plants were amplified by micropropagation as described by Behnke et al. (2007). To verify the level of transgenicity, qRT-PCR analysis was done on wild-type, vector control (pCambia), and RNAi (lines 2 and 9) plants. Primers for RNAi and qRT are given in Supplemental Table S2. MYB134-overexpressing lines of

P. tremula × *P. alba* (clone INRA 717-1B4) were available in the Constabel laboratory, propagated on Woody Plant Medium, and acclimated in a mist chamber before being moved to the greenhouse.

Statistical Analysis

All data were analyzed by using the statistical package R (version R 3.4.0). Before analysis, normality and homogeneity of variances were verified using Shapiro-Wilk and Levene's tests, respectively. Whenever necessary, data were square root or log transformed to meet the assumptions for parametric testing. Data were analyzed either by one-way or two-way ANOVA, depending on the overall number of factors in each experiment. Tukey's posthoc test was performed to compare differences among different groups.

Accession Numbers

Sequences used in this article can be found in the GenBank/EMBL/Phytozome libraries under the following accession numbers: MdLAR1 (DQ139836; *Malus domestica*), MdLAR2 (DQ139837; *Malus domestica*), PcLAR1 (DQ251190; *Pyrus communis*), PcLAR2 (DQ251191; *Pyrus communis*), FxaLAR1 (DQ834906; *Fragaria* × *ananassa*), VvLAR1 (BN000698; *Vitis vinifera*), VvLAR2 (3I6IA; *Vitis vinifera*), CsLAR (GU992401; *Camellia sinensis*), MtLAR (CAI56327.1; *Medicago truncatula*), LcLAR1 (DQ49103; *Lotus corniculatus*), LcLAR2 (DQ49105; *Lotus corniculatus*), PaLAR1 (KC589001; *Picea abies*), PaLAR2 (KC589002; *Picea abies*), PaLAR3 (KC589003; *Picea abies*), TcLAR (ADD51358; *Theobroma cacao*), GbANR (AAU95082; *Ginkgo biloba*), LcANR (ABC71337; *Lotus corniculatus*), TcANR (ADD51354; *Theobroma cacao*), FxaANR (ABG76842; *Fragaria* × *ananassa*), MtANR (AAN77735.1; *Medicago truncatula*), MdANR (AAZ79363; *Malus domestica*), CsANR1 (GU992402; *Camellia sinensis*), CsANR2 (GU992400; *Camellia sinensis*), PnLAR1 (KY751539; *Populus nigra*), PnLAR2 (KY751540; *Populus nigra*), PnLAR3 (KY751541; *Populus nigra*), PnANR1 (KY751542; *Populus nigra*), PnANR2 (KY751543; *Populus nigra*), and PtDFR1 (Potri.005G229500; *Populus trichocarpa*).

Supplemental Data

The following supplemental materials are available.

Supplemental Figure S1. Changes in poplar flavonoids and salicinoids during rust infection.

Supplemental Figure S2. Constitutive levels of flavan-3-ols and PAs in different tissues of 6-month-old black poplar (NP1) saplings.

Supplemental Figure S3. Transcript abundances of *LAR* and *ANR* genes catalyzing the last steps of flavan-3-ol biosynthesis in black poplar (NP1) saplings.

Supplemental Figure S4. Constitutive levels of salicinoids in different tissues of black poplar.

Supplemental Figure S5. Degrees of polymerization in poplar leaves and stems.

Supplemental Figure S6. Changes in the flavan-3-ol monomers epicatechin and gallocatechin in leaves of different poplar genotypes after 8 d of infection with rust fungus.

Supplemental Figure S7. Composition of flavan-3-ol monomers after hydrolysis of PAs in different poplar genotypes with or without rust infection.

Supplemental Figure S8. Relative abundances of *LAR* and *ANR* mRNA transcripts in water-treated control and rust-infected leaves of poplar genotypes 8 dpi.

Supplemental Figure S9. Illustration of in vitro bioassay with *M. larici-populina* on glass slides.

Supplemental Figure S10. Effects of different phenolic secondary metabolites on *M. larici-populina* spore germination in vitro.

Supplemental Figure S11. Silencing *PnMYB134*-regulating flavan-3-ols and PA biosynthesis in black poplar partially influenced other phenolic metabolites.

Supplemental Figure S12. Specificity of DMACA staining for different poplar phenolic metabolites.

Supplemental Figure S13. Alignment of the protein sequences.

Supplemental Table S1. Polar genotypes used for the rust (*M. larici-populina*) inoculation experiment under natural conditions.

Supplemental Table S2. List of primers used in this study.

ACKNOWLEDGMENTS

We thank Dr. Michael Reichelt for help with chemical analyses and Bettina Raguschke for assistance in the laboratory; Charlotte Lauder for work during her internship; all members of the greenhouse team, especially Andreas Weber, for growing hundreds of poplar plants used for this study; Richard Hamelin and Nicolas Feau for the *M. aecidiodes* spores; Jake Ketterer for help with plant care; the Northwest German Forest Research Station for providing stem cuttings of different poplar genotypes; and anonymous reviewers for their valuable comments and suggestions.

Received June 21, 2017; accepted October 23, 2017; published October 25, 2017.

LITERATURE CITED

Abeynayake SW, Panter S, Mouradov A, Spangenberg G (2011) A high-resolution method for the localization of proanthocyanidins in plant tissues. Plant Methods **7:** 13

Ayres MP, Clausen TP, MacLean SF, Redman AM, Reichardt PB (1997) Diversity of structure and anti-herbivore activity in condensed tannins. Ecology **78:** 1696–1712

Azaiez A, Boyle B, Levée V, Séguin A (2009) Transcriptome profiling in hybrid poplar following interactions with *Melampsora* rust fungi. Mol Plant Microbe Interact **22:** 190–200

Barbehenn RV, Constabel CP (2011) Tannins in plant-herbivore interactions. Phytochemistry **72:** 1551–1565

Barry KM, Davies NW, Mohammed CL (2002) Effect of season and different fungi on phenolics in response to xylem wounding and inoculation in *Eucalyptus nitens*. For Pathol **32:** 163–178

Behnke K, Ehlting B, Teuber M, Bauerfeind M, Louis S, Hänsch R, Polle A, Bohlmann J, Schnitzler JP (2007) Transgenic, non-isoprene emitting poplars don't like it hot. Plant J **51:** 485–499

Bennett RN, Wallsgrove RM (1994) Secondary metabolites in plant defence mechanisms. New Phytol **127:** 617–633

Boeckler GA, Gershenzon J, Unsicker SB (2011) Phenolic glycosides of the Salicaceae and their role as anti-herbivore defenses. Phytochemistry **72:** 1497–1509

Boeckler GA, Gershenzon J, Unsicker SB (2013) Gypsy moth caterpillar feeding has only a marginal impact on phenolic compounds in old-growth black poplar. J Chem Ecol **39:** 1301–1312

Boeckler GA, Towns M, Unsicker SB, Mellway RD, Yip L, Hilke I, Gershenzon J, Constabel CP (2014) Transgenic upregulation of the condensed tannin pathway in poplar leads to a dramatic shift in leaf palatability for two tree-feeding Lepidoptera. J Chem Ecol **40:** 150–158

Bogs J, Downey MO, Harvey JS, Ashton AR, Tanner GJ, Robinson SP (2005) Proanthocyanidin synthesis and expression of genes encoding leucoanthocyanidin reductase and anthocyanidin reductase in developing grape berries and grapevine leaves. Plant Physiol **139:** 652–663

Busby PE, Newcombe G, Dirzo R, Whitham TG (2013) Genetic basis of pathogen community structure for foundation tree species in a common garden and in the wild. J Ecol **101:** 867–877

Chen Z, Liang J, Zhang C, Rodrigues CJ Jr (2006) Epicatechin and catechin may prevent coffee berry disease by inhibition of appressorial melanization of *Colletotrichum kahawae*. Biotechnol Lett **28:** 1637–1640

Clavijo McCormick A, Irmisch S, Reinecke A, Boeckler GA, Veit D, Reichelt M, Hansson BS, Gershenzon J, Köllner TG, Unsicker SB (2014) Herbivore-induced volatile emission in black poplar: regulation and role in attracting herbivore enemies. Plant Cell Environ **37:** 1909–1923

Danielsson M, Lundén K, Elfstrand M, Hu J, Zhao T, Arnerup J, Ihrmark K, Swedjemark G, Borg-Karlson AK, Stenlid J (2011) Chemical and transcriptional responses of Norway spruce genotypes with different susceptibility to *Heterobasidion* spp. infection. BMC Plant Biol **11:** 154

Dardeau F, Deprost E, Laurans F, Lainé V, Lieutier F, Sallé A (2014) Resistant poplar genotypes inhibit pseudogall formation by the wooly poplar aphid, *Phloeomyzus passerinii* Sign. Trees **28:** 1007–1019

Debeaujon I, Nesi N, Perez P, Devic M, Grandjean O, Caboche M, Lepiniec L (2003) Proanthocyanidin-accumulating cells in *Arabidopsis* testa: regulation of differentiation and role in seed development. Plant Cell **15:** 2514–2531

de Colmenares NG, Ramírez-Martínez JR, Aldana JO, Ramos-Niño ME, Clifford MN, Pékerar S, Méndez B (1998) Isolation, characterisation and determination of biological activity of coffee proanthocyanidins. J Sci Food Agric **77:** 368–372

Dixon RA, Liu C, Jun JH (2013) Metabolic engineering of anthocyanins and condensed tannins in plants. Curr Opin Biotechnol **24:** 329–335

Dixon RA, Xie DY, Sharma SB (2005) Proanthocyanidins: a final frontier in flavonoid research? New Phytol **165:** 9–28

Duplessis S, Cuomo CA, Lin YC, Aerts A, Tisserant E, Veneault-Fourrey C, Joly DL, Hacquard S, Amselem J, Cantarel BL, et al (2011) Obligate biotrophy features unraveled by the genomic analysis of rust fungi. Proc Natl Acad Sci USA **108:** 9166–9171

Duplessis S, Major I, Martin F, Séguin A (2009) Poplar and pathogen interactions: insights from *Populus* genome-wide analyses of resistance and defense gene families and gene expression profiling. Crit Rev Plant Sci **28:** 309–334

Ferreira D, Slade D (2002) Oligomeric proanthocyanidins: naturally occurring O-heterocycles. Nat Prod Rep **19:** 517–541

Fischer TC, Halbwirth H, Meisel B, Stich K, Forkmann G (2003) Molecular cloning, substrate specificity of the functionally expressed dihydroflavonol 4-reductases from *Malus domestica* and *Pyrus communis* cultivars and the consequences for flavonoid metabolism. Arch Biochem Biophys **412:** 223–230

Guindon S, Dufayard JF, Lefort V, Anisimova M, Hordijk W, Gascuel O (2010) New algorithms and methods to estimate maximum-likelihood phylogenies: assessing the performance of PhyML 3.0. Syst Biol **59:** 307–321

Hacquard S, Petre B, Frey P, Hecker A, Rouhier N, Duplessis S (2011) The poplar-poplar rust interaction: insights from genomics and transcriptomics. J Pathogens **2011:** 716041

Hakulinen J, Sorjonen S, Julkunen-Tiitto R (1999) Leaf phenolics of three willow clones differing in resistance to *Melampsora* rust infection. Physiol Plant **105:** 662–669

Hammerbacher A, Paetz C, Wright LP, Fischer TC, Bohlmann J, Davis AJ, Fenning TM, Gershenzon J, Schmidt A (2014) Flavan-3-ols in Norway spruce: biosynthesis, accumulation, and function in response to attack by the bark beetle-associated fungus *Ceratocystis polonica*. Plant Physiol **164:** 2107–2122

Hammerbacher A, Schmidt A, Wadke N, Wright LP, Schneider B, Bohlmann J, Brand WA, Fenning TM, Gershenzon J, Paetz C (2013) A common fungal associate of the spruce bark beetle metabolizes the stilbene defenses of Norway spruce. Plant Physiol **162:** 1324–1336

Hemming JDC, Lindroth RL (1995) Intraspecific variation in aspen phytochemistry: effects on performance of gypsy moths and forest tent caterpillars. Oecologia **103:** 79–88

Henriquez MA, Adam LR, Daayf F (2012) Alteration of secondary metabolites' profiles in potato leaves in response to weakly and highly aggressive isolates of *Phytophthora infestans*. Plant Physiol Biochem **57:** 8–14

Irmisch S, Clavijo McCormick A, Günther J, Schmidt A, Boeckler GA, Gershenzon J, Unsicker SB, Köllner TG (2014) Herbivore-induced poplar cytochrome P450 enzymes of the CYP71 family convert aldoximes to nitriles which repel a generalist caterpillar. Plant J **80:** 1095–1107

Irmisch S, McCormick AC, Boeckler GA, Schmidt A, Reichelt M, Schneider B, Block K, Schnitzler JP, Gershenzon J, Unsicker SB, et al (2013) Two herbivore-induced cytochrome P450 enzymes CYP79D6 and CYP79D7 catalyze the formation of volatile aldoximes involved in poplar defense. Plant Cell **25:** 4737–4754

Jansson S, Douglas CJ (2007) *Populus*: a model system for plant biology. Annu Rev Plant Biol **58:** 435–458

Jun JH, Liu C, Xiao X, Dixon RA (2015) The transcriptional repressor MYB2 regulates both spatial and temporal patterns of proanthocyanidin and anthocyanin pigmentation in *Medicago truncatula*. Plant Cell **27:** 2860–2879

Kao YY, Harding SA, Tsai CJ (2002) Differential expression of two distinct phenylalanine ammonia-lyase genes in condensed tannin-accumulating and lignifying cells of quaking aspen. Plant Physiol **130:** 796–807

Katoh K, Standley DM (2013) MAFFT multiple sequence alignment software version 7: improvements in performance and usability. Mol Biol Evol **30:** 772–780

Kelm MA, Johnson JC, Robbins RJ, Hammerstone JF, Schmitz HH (2006) High-performance liquid chromatography separation and purification of cacao (*Theobroma cacao* L.) procyanidins according to degree of polymerization using a diol stationary phase. J Agric Food Chem **54:** 1571–1576

Koskimäki JJ, Hokkanen J, Jaakola L, Suorsa M, Tolonen A, Mattila S, Pirttilä AM, Hohtola A (2009) Flavonoid biosynthesis and degradation play a role in early defence responses of bilberry (*Vaccinium myrtillus*) against biotic stress. Eur J Plant Pathol **125:** 629–640

Kosonen M, Keski-Saari S, Ruuhola T, Constabel CP, Julkunen-Tiitto R (2012) Effects of overproduction of condensed tannins and elevated temperature on chemical and ecological traits of genetically modified hybrid aspens (*Populus tremula* × *P. tremuloides*). J Chem Ecol **38:** 1235–1246

Kutchan T, Gershenzon J, Moller BL, Gang D (2015) Natural products. *In* BB Buchanan, W Gruissem, RL Jones, eds, Biochemistry and Molecular Biology of Plants. John Wiley & Sons, Oxford, pp 1132–1206

Lattanzio V, Lattanzio VM, Cardinali A (2006) Role of phenolics in the resistance mechanisms of plants against fungal pathogens and insects. Phytochemistry **661:** 23–67

Le SQ, Gascuel O (2008) An improved general amino acid replacement matrix. Mol Biol Evol **25:** 1307–1320

Levée V, Major I, Levasseur C, Tremblay L, MacKay J, Séguin A (2009) Expression profiling and functional analysis of *Populus* WRKY23 reveals a regulatory role in defense. New Phytol **184:** 48–70

Liao L, Vimolmangkang S, Wei G, Zhou H, Korban SS, Han Y (2015) Molecular characterization of genes encoding leucoanthocyanidin reductase involved in proanthocyanidin biosynthesis in apple. Front Plant Sci **6:** 243

Lindroth RL, Hwang SY (1996) Diversity, redundancy, and multiplicity in chemical defense systems of aspen. *In* JT Romeo, JA Saunders, P Barbosa, eds, Phytochemical Diversity and Redundancy in Ecological Interactions. Plenum Press, New York, pp 25–56

Liu C, Wang X, Shulaev V, Dixon RA (2016) A role for leucoanthocyanidin reductase in the extension of proanthocyanidins. Nat Plants **2:** 16182

Massad TJ, Trumbore SE, Ganbat G, Reichelt M, Unsicker S, Boeckler A, Gleixner G, Gershenzon J, Ruehlow S (2014) An optimal defense strategy for phenolic glycoside production in *Populus trichocarpa*: isotope labeling demonstrates secondary metabolite production in growing leaves. New Phytol **203:** 607–619

Meilan R, Ma C (2006) Populus. Methods Mol Biol **344:** 143–152

Mellway RD, Tran LT, Prouse MB, Campbell MM, Constabel CP (2009) The wound-, pathogen-, and ultraviolet B-responsive MYB134 gene encodes an R2R3 MYB transcription factor that regulates proanthocyanidin synthesis in poplar. Plant Physiol **150:** 924–941

Miranda M, Ralph SG, Mellway R, White R, Heath MC, Bohlmann J, Constabel CP (2007) The transcriptional response of hybrid poplar (*Populus trichocarpa* × *P. deltoides*) to infection by *Melampsora medusae* leaf rust involves induction of flavonoid pathway genes leading to the accumulation of proanthocyanidins. Mol Plant Microbe Interact **20:** 816–831

Nemesio-Gorriz M, Hammerbacher A, Ihrmark K, Källman T, Olson Å, Lascoux M, Stenlid J, Gershenzon J, Elfstrand M (2016) Different alleles of a gene encoding leucoanthocyanidin reductase (PaLAR3) influence resistance against the fungus *Heterobasidion parviporum* in *Picea abies*. Plant Physiol **171:** 2671–2681

Newcombe G (1996) The specificity of fungal pathogens of *Populus*. *In* RF Stettler, HD Bradshaw, PE. Heolman, TM Hinckley, eds, Biology of *Populus* and Its Implications for Management and Conservation. NRC Research Press, Ottawa, Canada, pp 223–246

Newcombe G, Ostry M, Hubbes M, P'erinet P, Mottet MJ (2001) Poplar diseases. *In* DI Dickmann, JG Isebrands, JE Eckenwalder, J Richardson, eds, Poplar Culture in North America. NRC Research Press, Ottawa, Canada, pp 249–276

O'Maille PE, Tsai MD, Greenhagen BT, Chappell J, Noel JP (2004) Gene library synthesis by structure-based combinatorial protein engineering. Methods Enzymol **388:** 75–91

Osbourn AE (1996) Preformed antimicrobial compounds and plant defense against fungal attack. Plant Cell **8:** 1821–1831

Palo RT (1984) Distribution of birch (*Betula* spp.), willow (*Salix* spp.), and poplar (*Populus* spp.) secondary metabolites and their potential role as chemical defense against herbivores. J Chem Ecol **10:** 499–520

Pang Y, Abeysinghe IS, He J, He X, Huhman D, Mewan KM, Sumner LW, Yun J, Dixon RA (2013) Functional characterization of proanthocyanidin pathway enzymes from tea and their application for metabolic engineering. Plant Physiol **161:** 1103–1116

Paolocci F, Robbins MP, Madeo L, Arcioni S, Martens S, Damiani F (2007) Ectopic expression of a basic helix-loop-helix gene transactivates parallel pathways of proanthocyanidin biosynthesis: structure, expression analysis, and genetic control of leucoanthocyanidin 4-reductase and anthocyanidin reductase genes in *Lotus corniculatus*. Plant Physiol **143:** 504–516

Pearl IA, Darling SF (1971) Phenolic extractives of the leaves of *Populus balsamifera* and of *P. trichocarpa*. Phytochemistry **10:** 2844–2847

Pereira D, Valentão P, Pereira J, Andrade P (2009) Phenolics: from chemistry to biology. Molecules **14:** 2202

Peters DJ, Constabel CP (2002) Molecular analysis of herbivore-induced condensed tannin synthesis: cloning and expression of dihydroflavonol reductase from trembling aspen (*Populus tremuloides*). Plant J **32:** 701–712

Pfabel C, Eckhardt KU, Baum C, Struck C, Frey P, Weih M (2012) Impact of ectomycorrhizal colonization and rust infection on the secondary metabolism of poplar (*Populus trichocarpa* × *deltoides*). Tree Physiol **32:** 1357–1364

Porter LJ, Hrstich LN, Chan BG (1985) The conversion of procyanidins and prodelphinidins to cyanidin and delphinidin. Phytochemistry **25:** 223–230

Prithiviraj B, Perry LG, Badri DV, Vivanco JM (2007) Chemical facilitation and induced pathogen resistance mediated by a root-secreted phytotoxin. New Phytol **173:** 852–860

Robinson BH, Mills TM, Petit D, Fung LE, Green SR, Clothier BE (2000) Natural and induced cadmium-accumulation in poplar and willow: implications for phytoremediation. Plant Soil **227:** 301–306

Schnoor JL, Licht LA, McCutcheon SC, Wolfe NL, Carreira LH (1995) Phytoremediation of organic and nutrient contaminants. Environ Sci Technol **29:** 318A–323A

Stanturf JA, Van Oosten C, Netzer DA, Coleman MD, Portwood CJ (2001) Ecology and silviculture of poplar plantations. *In* DI Dickmann, JG Isebrands, JE Eckenwalder, J Richardson, eds, Poplar Culture in North America. NRC Research Press, Ottawa, Canada, pp 153–206

Tanner GJ, Francki KT, Abrahams S, Watson JM, Larkin PJ, Ashton AR (2003) Proanthocyanidin biosynthesis in plants: purification of legume leucoanthocyanidin reductase and molecular cloning of its cDNA. J Biol Chem **278:** 31647–31656

Treutter D (2005) Significance of flavonoids in plant resistance and enhancement of their biosynthesis. Plant Biol (Stuttg) **7:** 581–591

Tsai CJ, Harding SA, Tschaplinski TJ, Lindroth RL, Yuan Y (2006) Genome-wide analysis of the structural genes regulating defense phenylpropanoid metabolism in Populus. New Phytol **172:** 47–62

Tuskan GA, Difazio S, Jansson S, Bohlmann J, Grigoriev I, Hellsten U, Putnam N, Ralph S, Rombauts S, Salamov A, et al (2006) The genome of black cottonwood, *Populus trichocarpa* (Torr. & Gray). Science **313:** 1596–1604

Vandeputte OM, Kiendrebeogo M, Rajaonson S, Diallo B, Mol A, El Jaziri M, Baucher M (2010) Identification of catechin as one of the flavonoids from *Combretum albiflorum* bark extract that reduces the production of quorum-sensing-controlled virulence factors in *Pseudomonas aeruginosa* PAO1. Appl Environ Microbiol **76:** 243–253

Wang L, Jiang Y, Yuan L, Lu W, Yang L, Karim A, Luo K (2013) Isolation and characterization of cDNAs encoding leucoanthocyanidin reductase and anthocyanidin reductase from *Populus trichocarpa*. PLoS ONE **8:** e64664

Wang L, Ran L, Hou Y. Tian Q, Li C, Liu R, Fan D, Luo K (2017) The transcription factor MYB115 contributes to the regulation of proanthocyanidin biosynthesis and enhances fungal resistance in poplar. New Phytol **215:** 351–367

Whitham TG, Bailey JK, Schweitzer JA, Shuster SM, Bangert RK, LeRoy CJ, Lonsdorf EV, Allan GJ, DiFazio SP, Potts BM, et al (2006) A framework for community and ecosystem genetics: from genes to ecosystems. Nat Rev Genet **7:** 510–523

Xie DY, Sharma SB, Dixon RA (2004) Anthocyanidin reductases from *Medicago truncatula* and *Arabidopsis thaliana*. Arch Biochem Biophys **422:** 91–102

Yamaji K, Ichihara Y (2012) The role of catechin and epicatechin in chemical defense against damping-off fungi of current-year Fagus crenata seedlings in natural forest. For Pathol **42:** 1–7

Yoshida K, Ma D, Constabel CP (2015) The MYB182 protein down-regulates proanthocyanidin and anthocyanin biosynthesis in poplar by repressing both structural and regulatory flavonoid genes. Plant Physiol **167:** 693–710

Yuan L, Wang L, Han Z, Jiang Y, Zhao L, Liu H, Yang L, Luo K (2012) Molecular cloning and characterization of *PtrLAR3*, a gene encoding leucoanthocyanidin reductase from *Populus trichocarpa*, and its constitutive expression enhances fungal resistance in transgenic plants. J Exp Bot **63:** 2513–2524

Zhang Y, De Stefano R, Robine M, Butelli E, Bulling K, Hill L, Rejzek M, Martin C, Schoonbeek HJ (2015) Different reactive oxygen species scavenging properties of flavonoids determine their abilities to extend the shelf life of tomato. Plant Physiol **169:** 1568–1583